SIGGRAPH 2020 S2020.SIGGRAPH.ORG THINK BEYOND

SAND2020-7297C

VOROCRUST

VORONOI MESHING WITHOUT CLIPPING

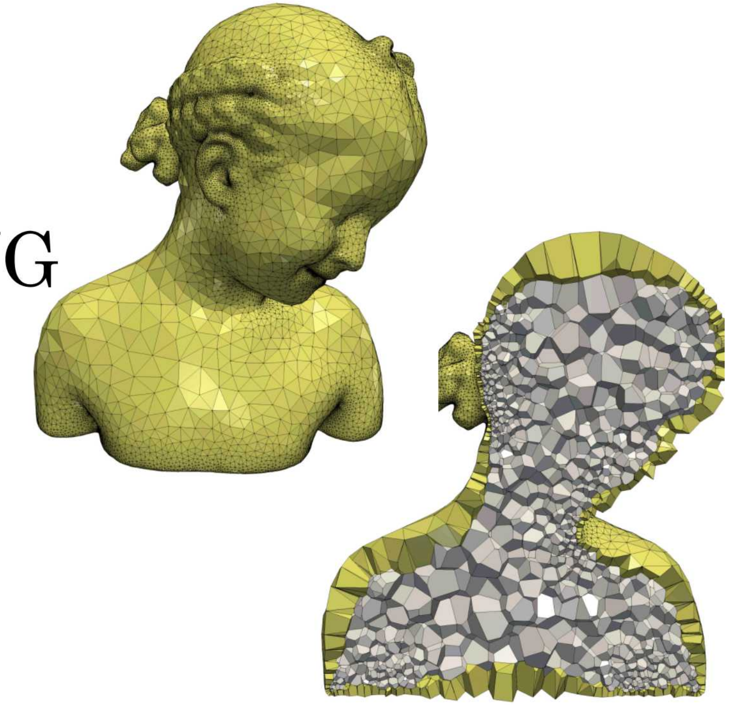

Ahmed Abdelkader[1], Chandrajit Bajaj[2], Mohamed Ebeida[3], Ahmed Mahmoud[4], Scott Mitchell[3], John D. Owens[4], and Ahmad Rushdi[3]

[1]University of Maryland, College Park; [2]University of Texas, Austin; [3]Sandia National Laboratories, Albuquerque; [4]University of California, Davis

Sandia National Laboratories is a multimission laboratory managed and operated by National Technology & Engineering Solutions of Sandia, LLC, a wholly owned subsidiary of Honeywell International Inc., for the U.S. Department of Energy's National Nuclear Security Administration under contract DE-NA0003525.

What is a Voronoi mesh?

Given a set of points (seeds), a Voronoi cell is formed around each seed by the set of points that are closest to that seed compared to any other seed.

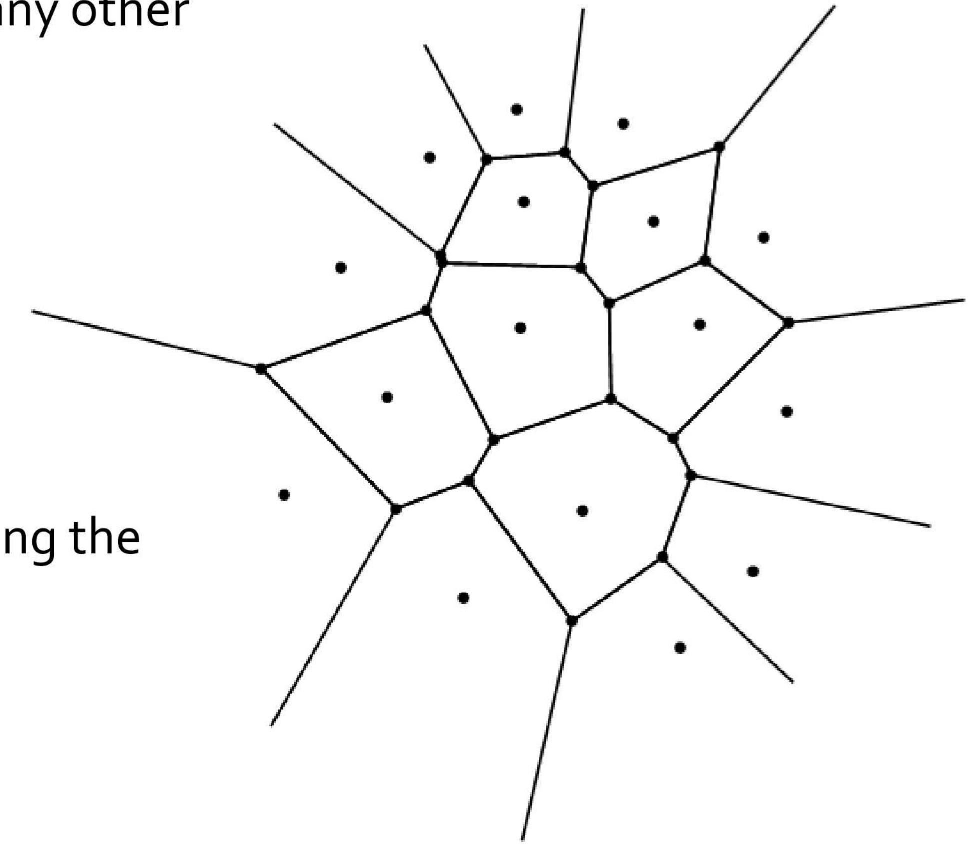

Direct implications:

- Each cell is convex
- Each cell is bounded by planar convex facets
- A facet between two cells is orthogonal to the line connecting the cell seeds

Main Challenge:

- Representing (external and internal) boundaries is a hard problem.

Polyhedral, Tetrahedral, and Hexahedral Mesh Comparison

Source: https://meshing.lanl.gov/proj/SFWD_models/main.html

- Polyhedral meshing is important for flow and transport codes which include TOUGH2, FEHM, PFLOTRAN, and MODFLOW which are based on the two-point flux discretization

- While the solution to flow/transport is stable without an orthogonal mesh, it is not accurate!

- A well-principled framework is enabled through the combined use of primal meshes and their orthogonal duals [Mullen et al. 2011].

- The power of orthogonal duals, exemplified by Voronoi-Delaunay meshes, has recently been demonstrated on a range of applications in computer graphics [Goes et al. 2014] and computational physics [Engwirda 2018].

- It is therefore imperative to develop new algorithms for
- primal-dual polyhedral meshing

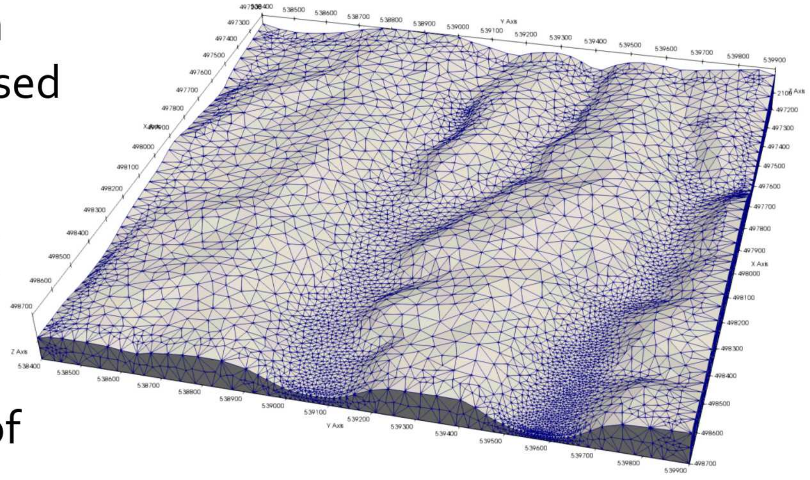

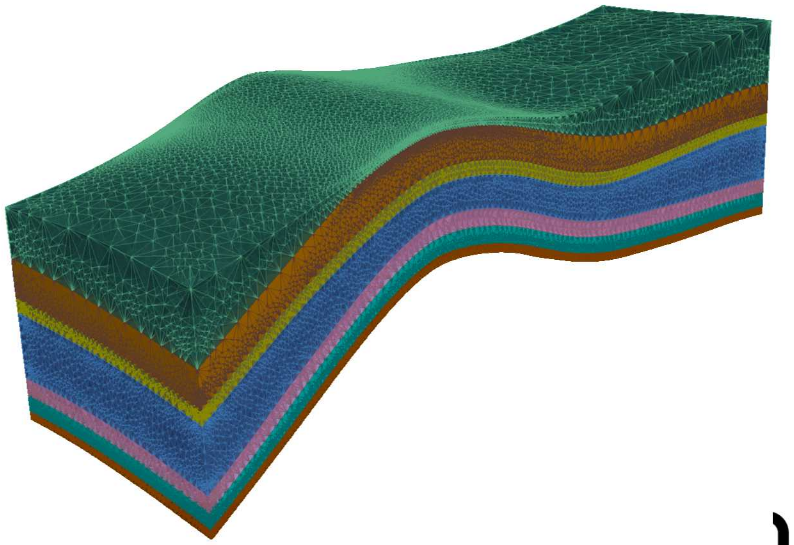

Polyhedral, Tetrahedral, and Hexahedral Mesh Comparison

Source: https://www.symscape.com/

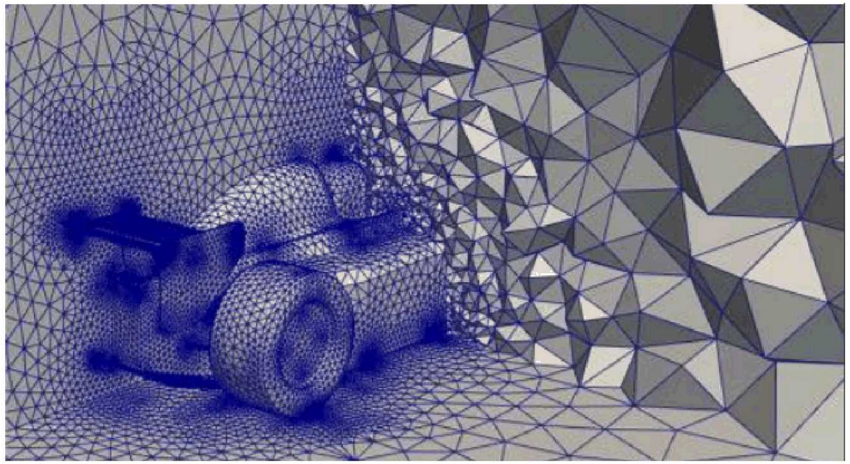

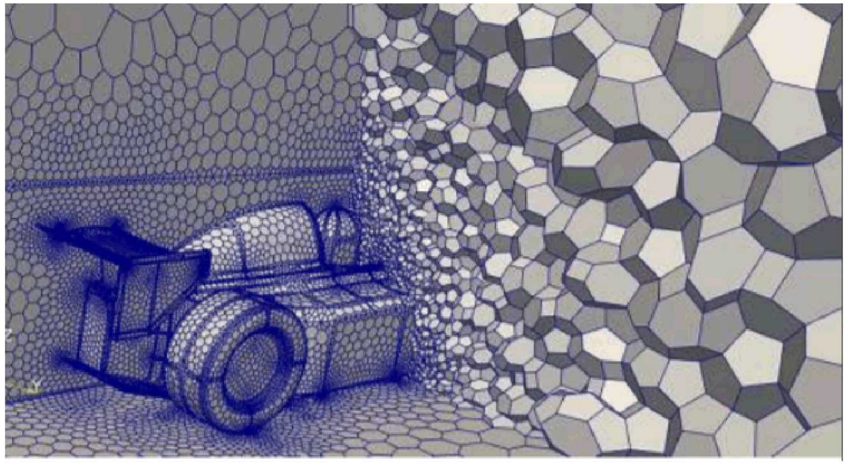

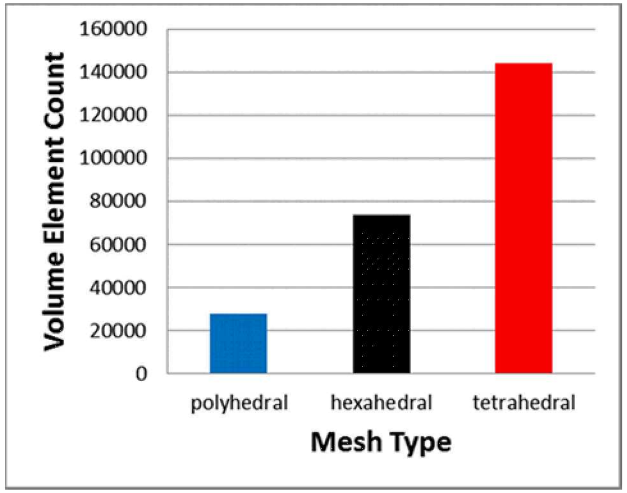

Fewer Elements

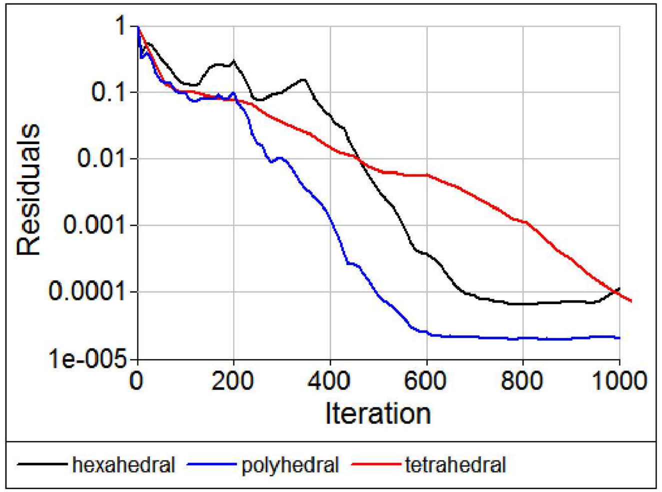

Robust Convergence

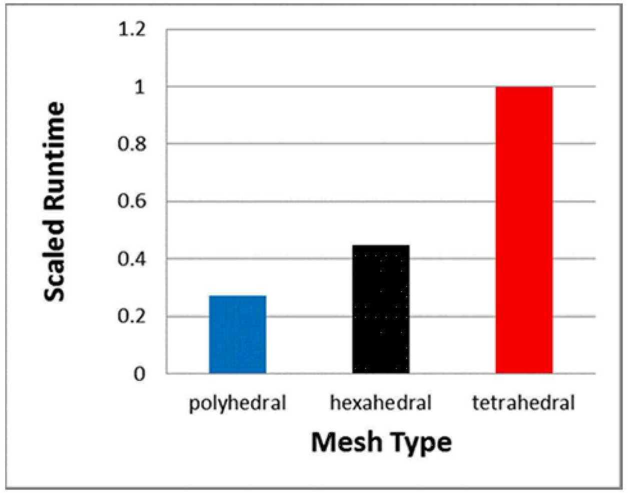

Faster Simulation Runtime

Current approaches for representing boundaries

Clipping:

- Confine the Voronoi diagram to a compact domain.

Direct implications:

- Clipped cell may loose convexity and orphan cells may be generated
- Boundary facets could be non-planar and may have poor quality.
- The orthogonality property is no longer maintained
- It is not clear how to robustly represent internal interfaces.

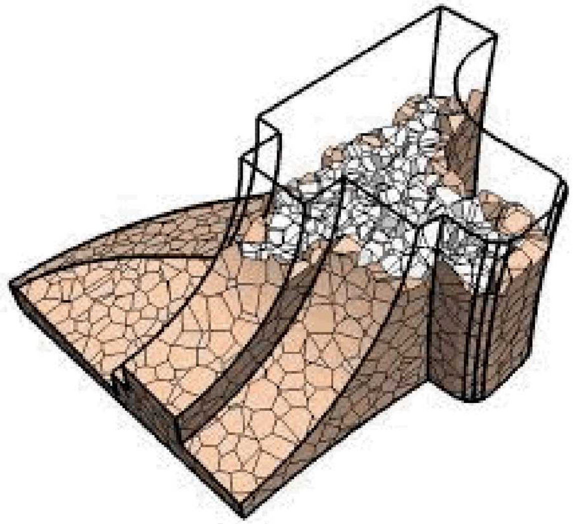

Efficient Computation of 3D Clipped Voronoi Diagram
Yan D. M. et. al. [2010]

Uniform Random Voronoi Meshes
Ebeida M. S. and Mitchell S. A. [2011]

Current approaches for representing boundaries

Naive Mirroring:

- Mirror the seeds across the boundary

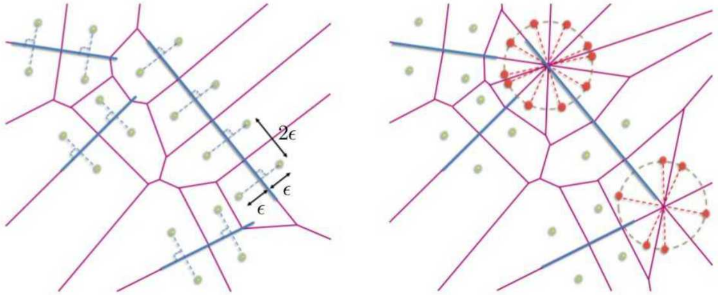

Pros:

- No clipping, resulting cells are convex, bounded by planar facets

Cons:

- Curved Boundaries result in bad normal

  → Noisy surface approximation

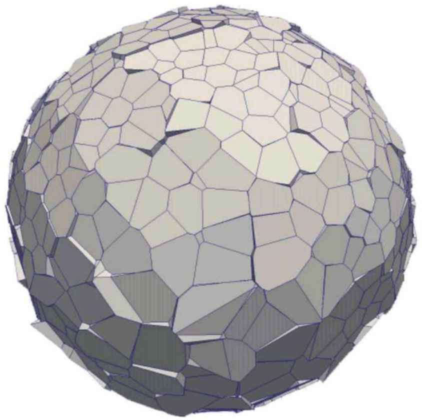

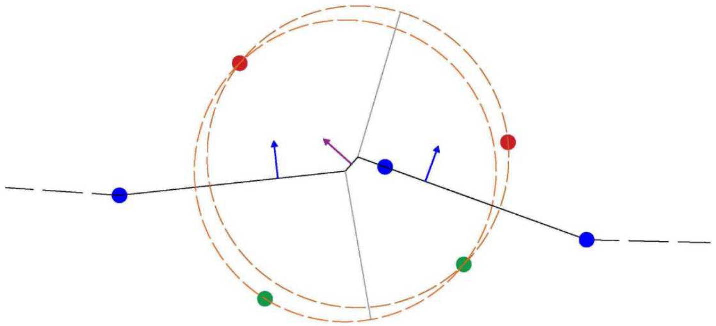

Smart Mirroring:

- We eliminated all the facets that have bad normal by forcing the pairs of neighbor mirror seeds to lie on the same Delaunay sphere → undesired facets become degenerate.

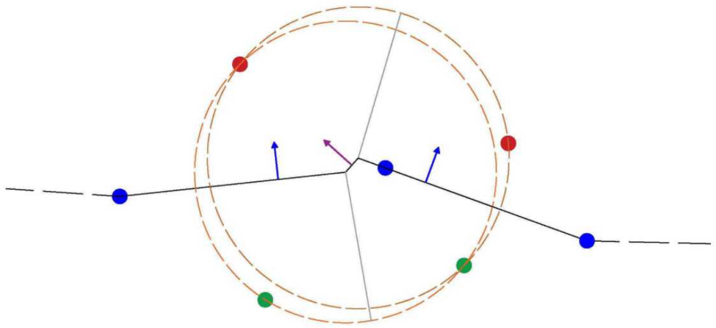

How?

- We cover the surface with spheres and place the seeds at the intersection pair of these spheres.

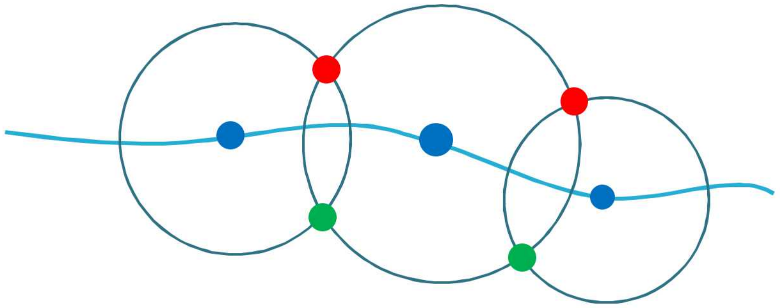

Our approach (a simple illustration)

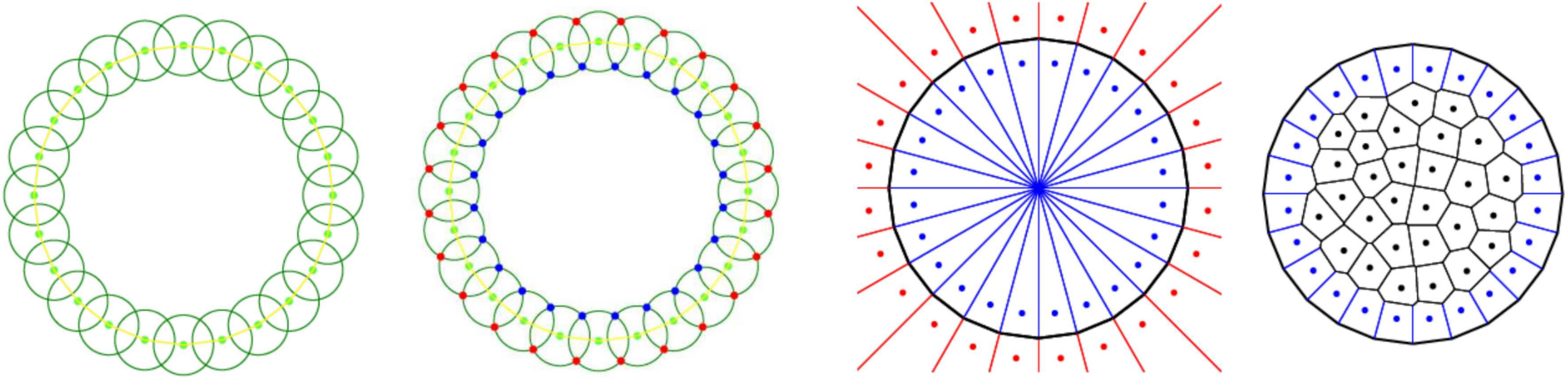

1. Cover input model with spheres

2. Place Voronoi seeds at the intersection pairs

3. Reconstruct the boundaries

4. Add interior seeds to improve mesh quality

Our approach: Questions that we had to answer

1. How to automatically choose the radii of surface spheres?
2. How to achieve (and maintain) maximal coverage efficiently?
3. In 3D, there could be an intersection pair of three surface spheres, where one point is covered and the other is not. How do we handle this situation?
4. How to detect and represent sharp features (sharp corners and sharp curves).
5. How to handle internal interfaces and domains with multiple materials?

Our next speaker will now present our answers.

Our approach (a simple illustration in 3D)

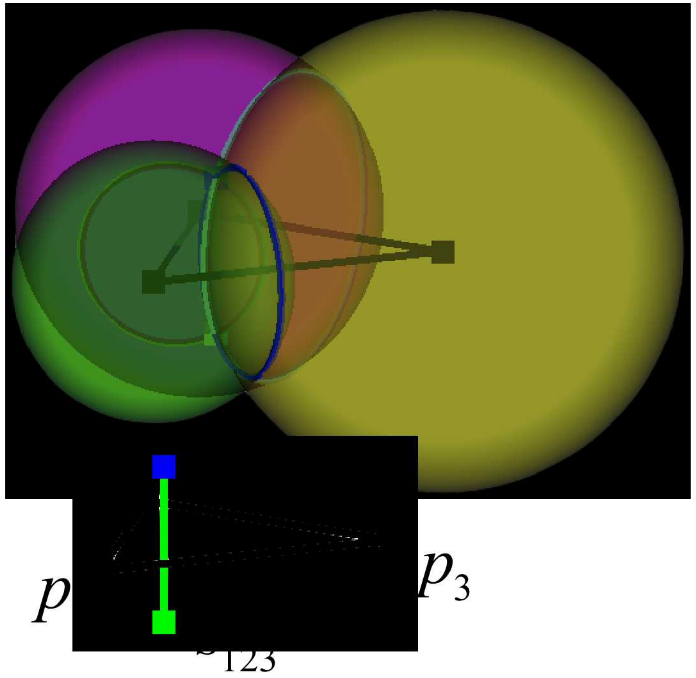

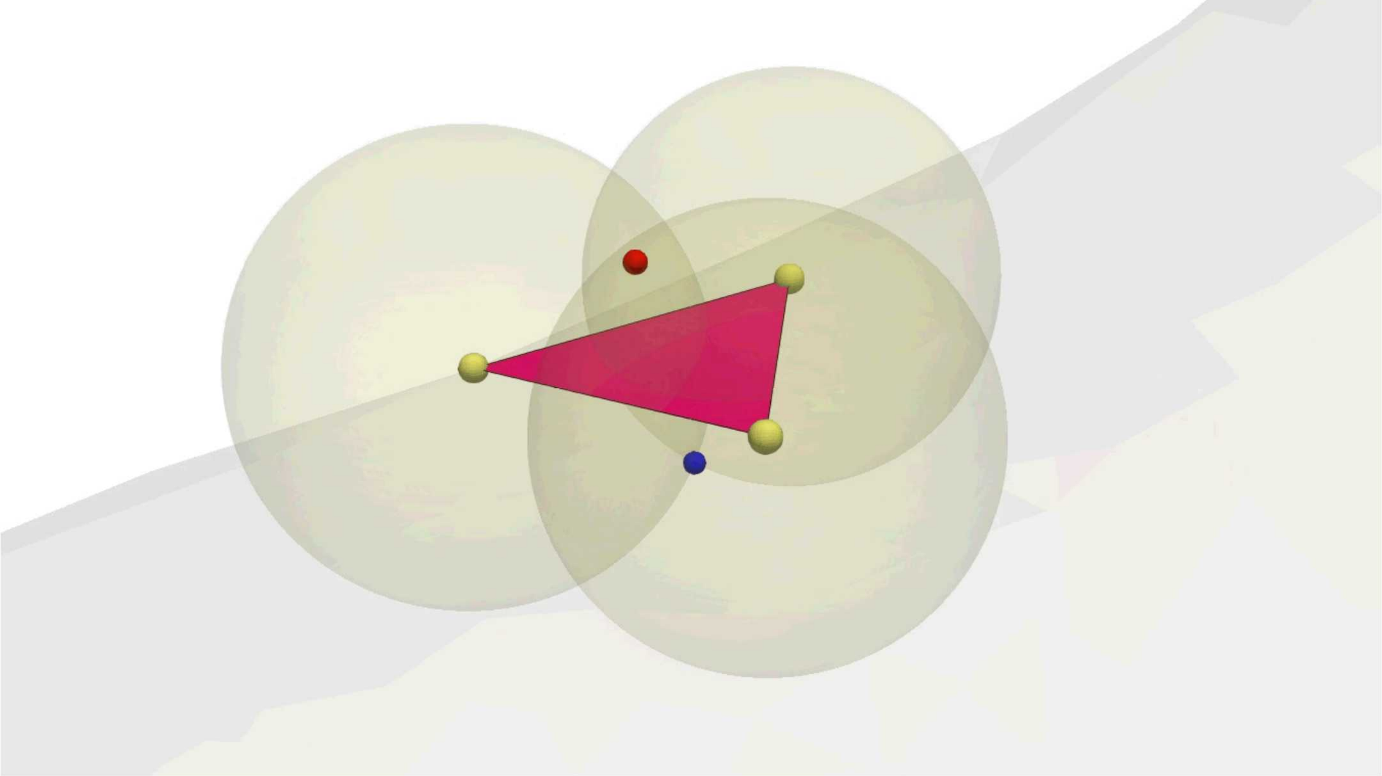

Sampling Conditions for Reconstruction [SoCG'18]

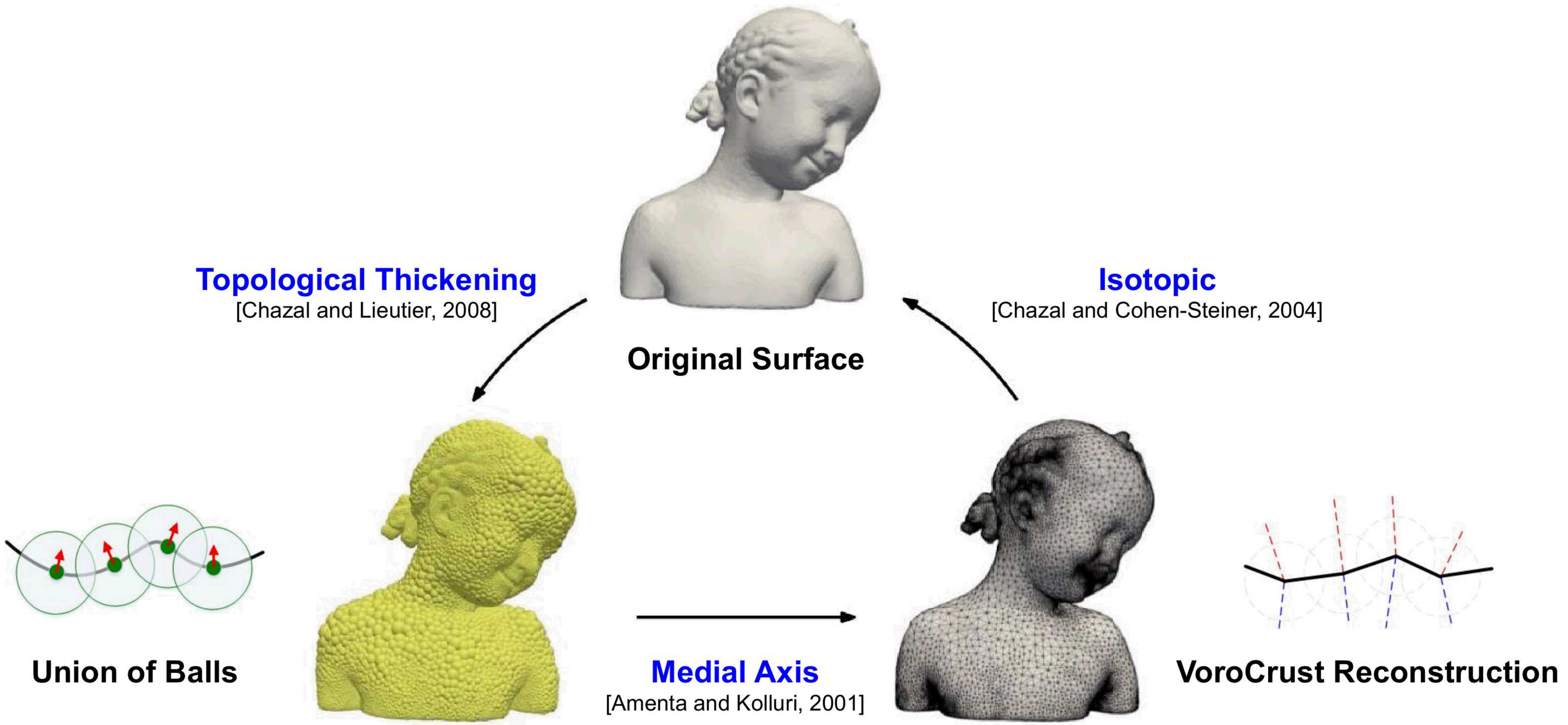

VoroCrust Refinement

Input:

- T: an accurate surface approximation
- $\theta^{\#}$: threshold to identify sharp features

Requirements:

- Generate union of balls
- Additional conditions for quality

Ball Conditions:

- Smooth coverage ($\theta^{\#}$)
- Smooth overlaps
- Locally Lipschitz (L)
- Deep coverage with sparsity (α)

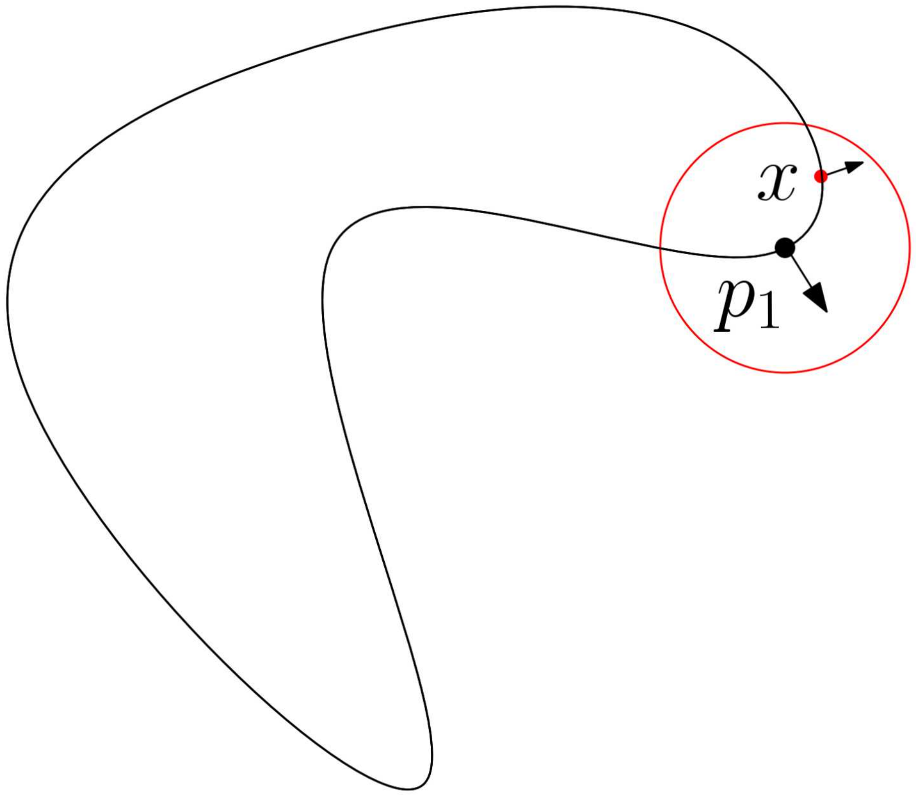

Ball Conditions:

- Smooth coverage ($\theta^{\#}$)
- Smooth overlaps
- Locally Lipschitz (L)
- Deep coverage with sparsity (α)

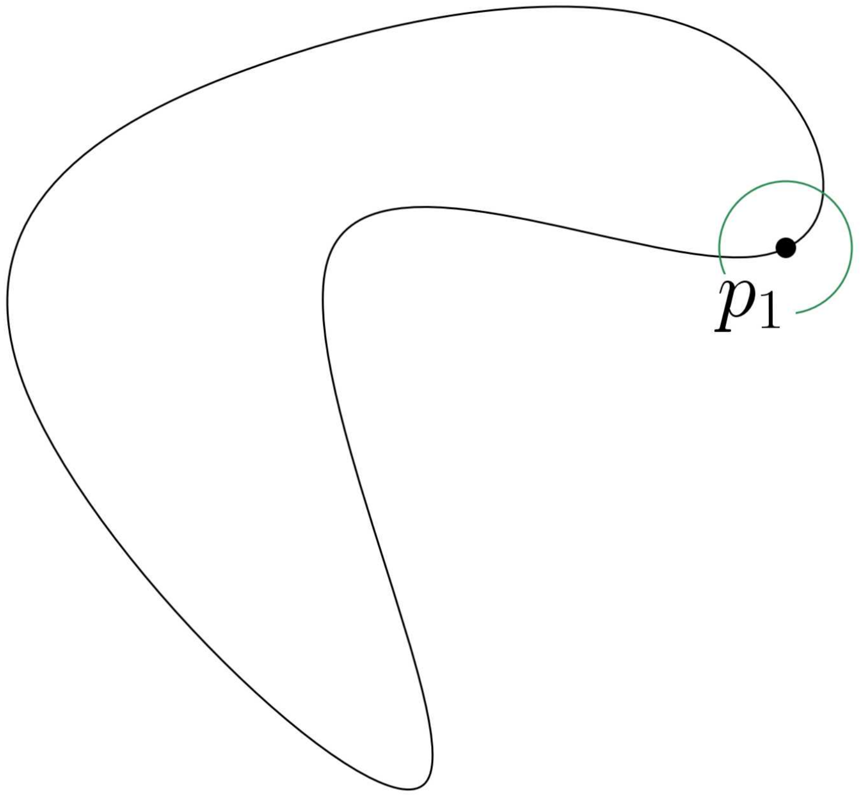

Ball Conditions:

- Smooth coverage ($\theta^{\#}$)
- Smooth overlaps
- Locally Lipschitz (L)
- Deep coverage with sparsity (α)

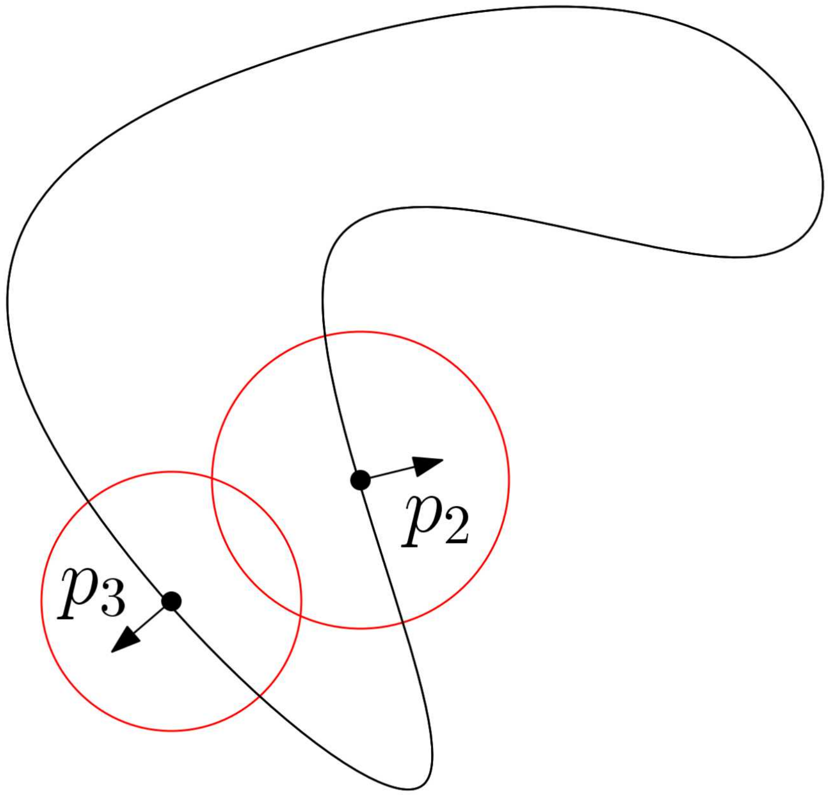

Ball Conditions:

- Smooth coverage ($\theta^{\#}$)
- Smooth overlaps
- Locally Lipschitz (L)
- Deep coverage with sparsity (α)

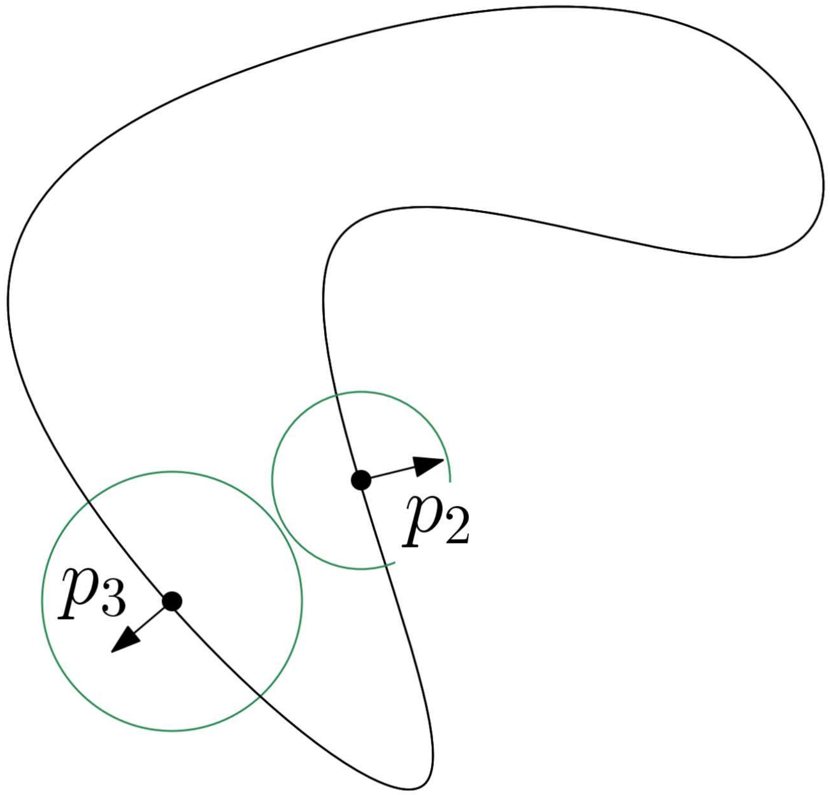

VoroCrust Refinement

Ball Conditions:

- Smooth coverage ($\theta^{\#}$)
- Smooth overlaps
- Locally Lipschitz (L)
- Deep coverage with sparsity (α)

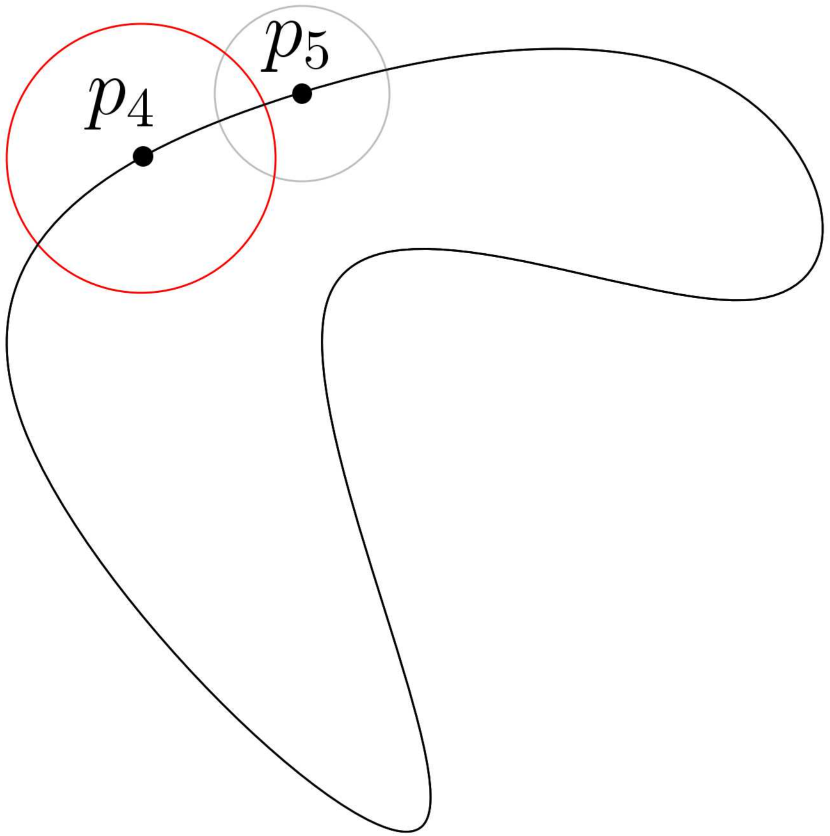

Ball Conditions:

- Smooth coverage ($\theta^{\#}$)
- Smooth overlaps
- Locally Lipschitz (L)
- Deep coverage with sparsity (α)

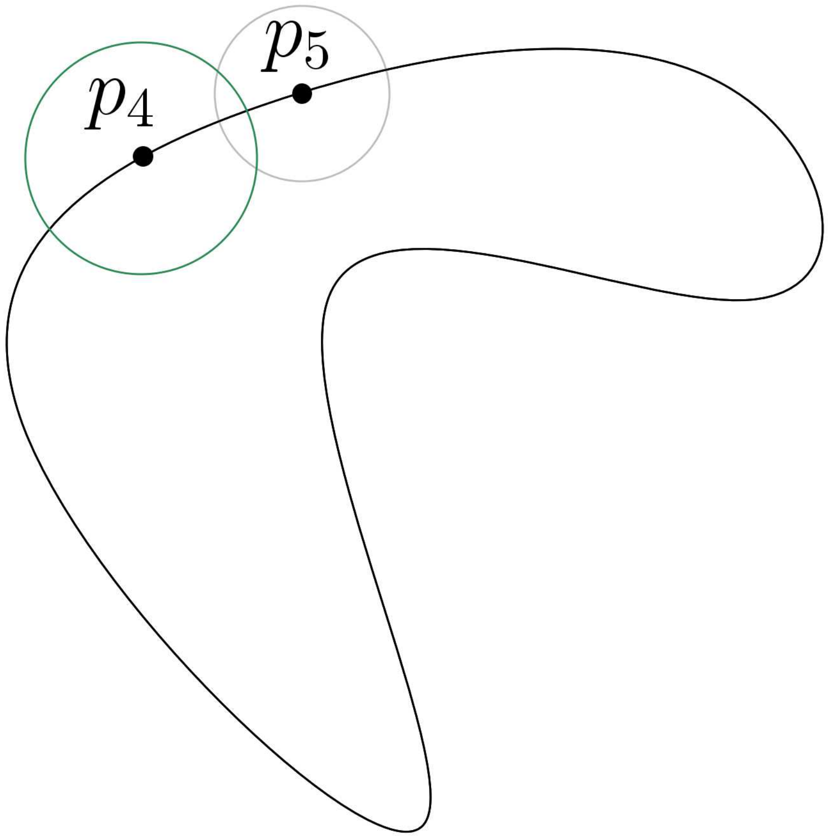

Ball Conditions:

- Smooth coverage ($\theta^{\#}$)
- Smooth overlaps
- Locally Lipschitz (L)
- Deep coverage with sparsity (α)

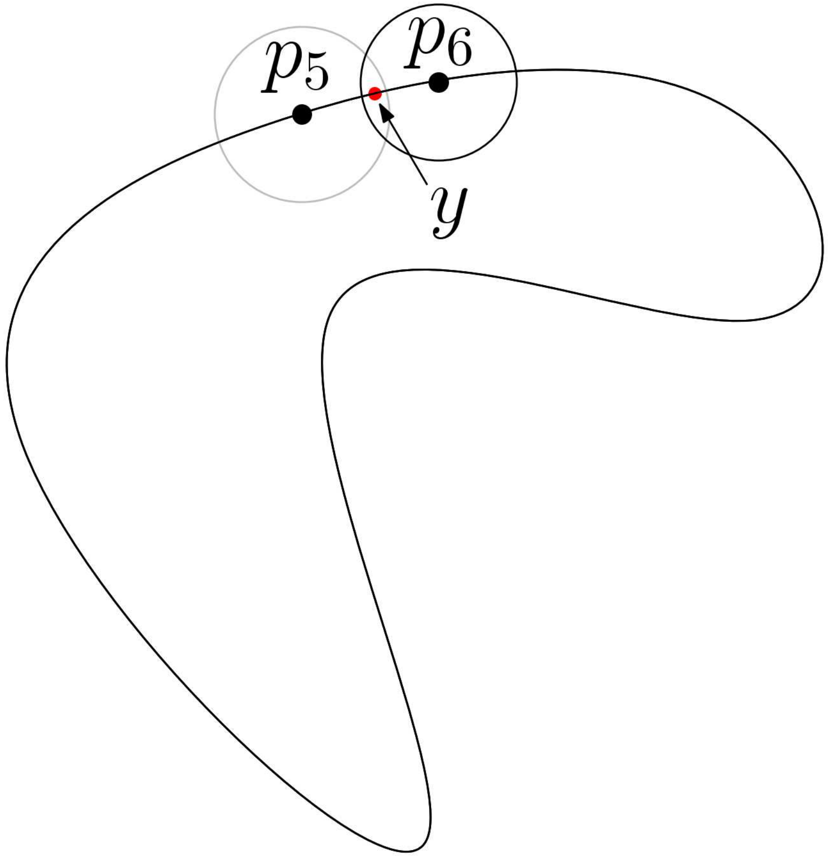

Ball Conditions:

- Smooth coverage ($\theta^{\#}$)
- Smooth overlaps
- Locally Lipschitz (L)
- Deep coverage with sparsity (α)

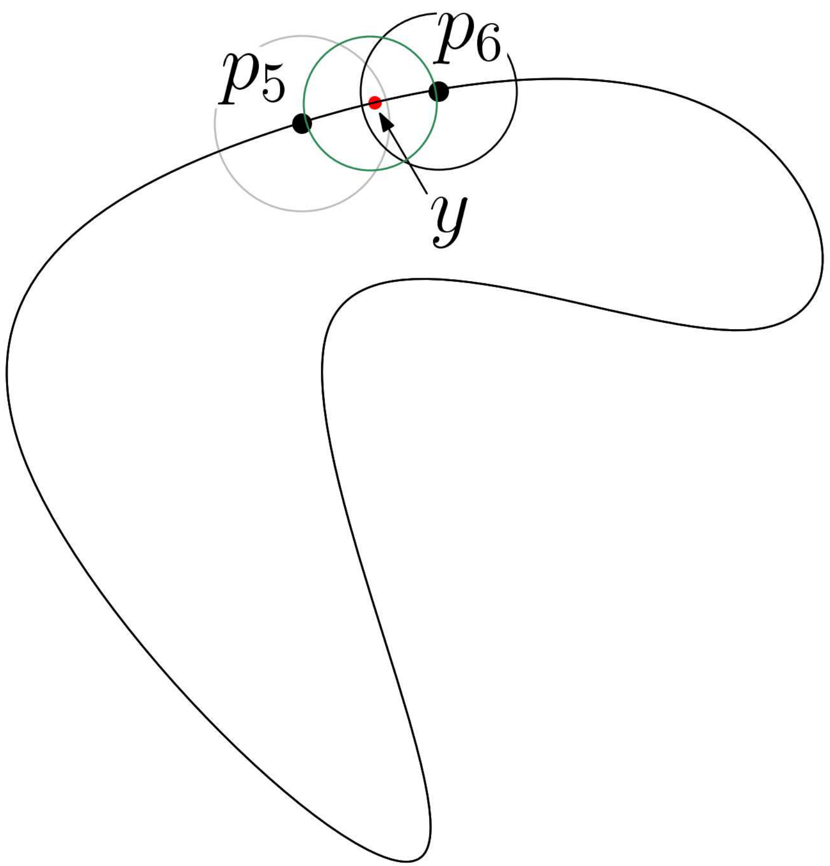

VoroCrust Refinement

Ball Conditions:

- Smooth coverage ($\theta^{\#}$)
- Smooth overlaps
- Locally Lipschitz (L)
- Deep coverage with sparsity (α)

Violations resolved by shrinking

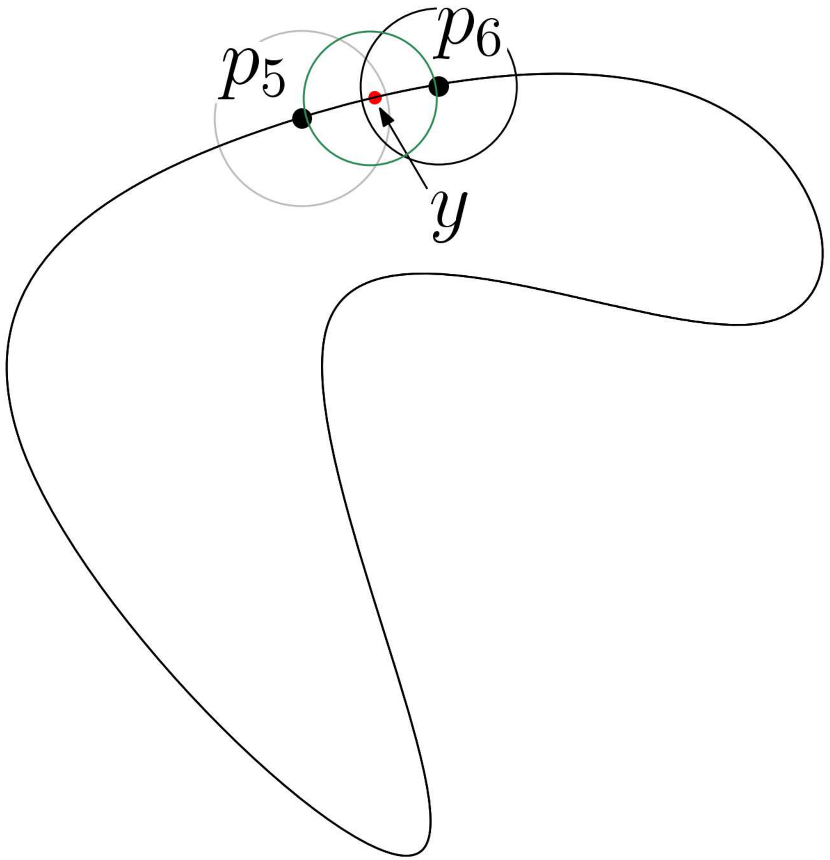

VoroCrust Refinement Loop (simplified)

Algorithm 1: High-level VoroCrust algorithm

Input: Triangle mesh $\mathcal{T}$, and parameters $\theta^\sharp$ and L

$\mathcal{B} \leftarrow \emptyset$
while $\mathcal{U} = \cup\mathcal{B}$ *does not cover* $\mathcal{T}$ **do**
    Add balls to cover $\mathcal{T}$
    Shrink balls violating any ball conditions
end
$\mathcal{S}^\updownarrow \leftarrow$ pairs of seeds from triplets of balls in $\mathcal{B}$
return $\mathcal{S}^\updownarrow$

Surface Coverage with Sharp Feature Protection

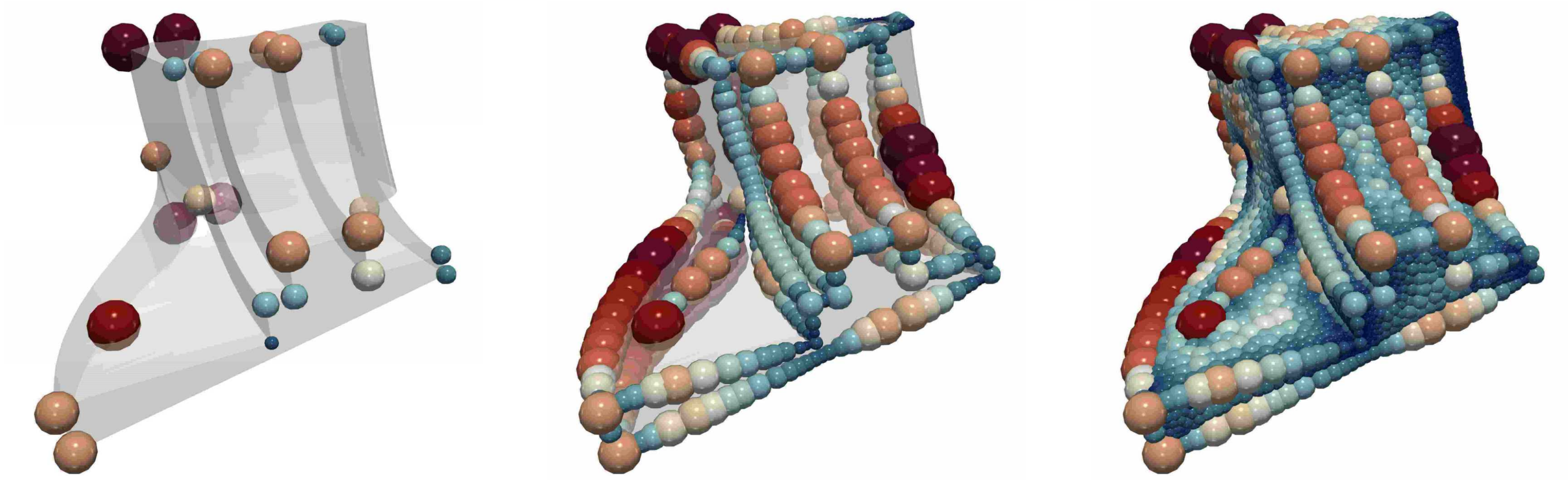

Corner balls ⇔ Edge balls ⇔ Surface balls

Surface Defects

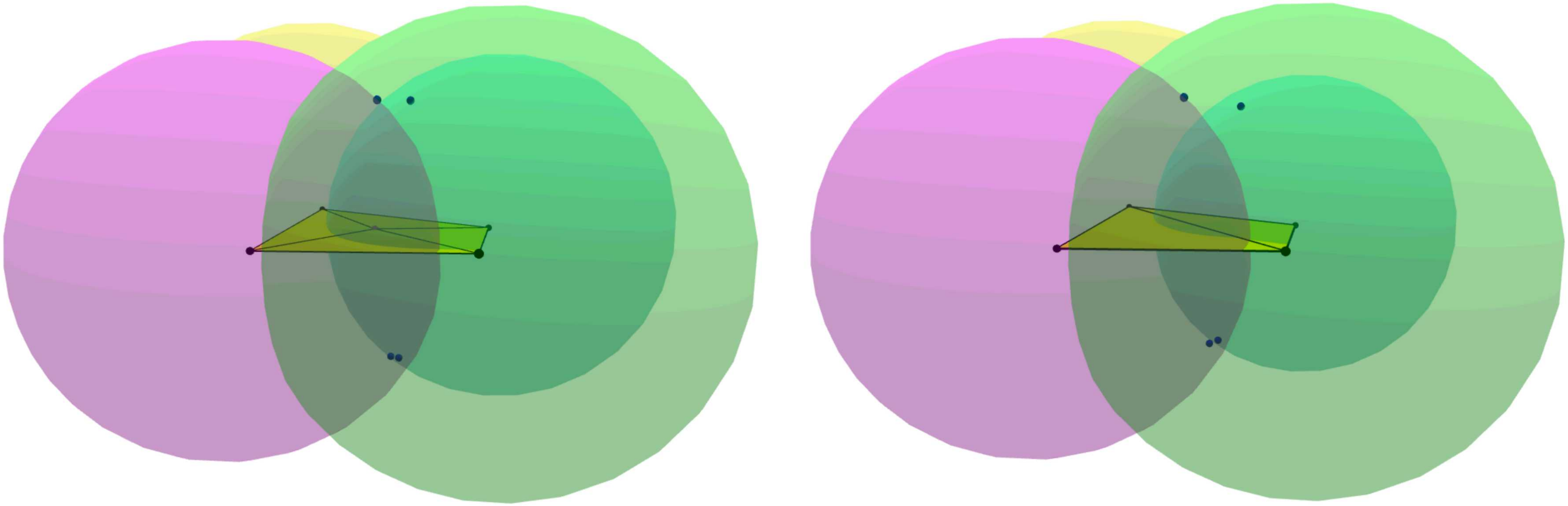

Extra Steiner vertex (sliver) ⇒ No sliver after perturbation of radii

Surface Defects

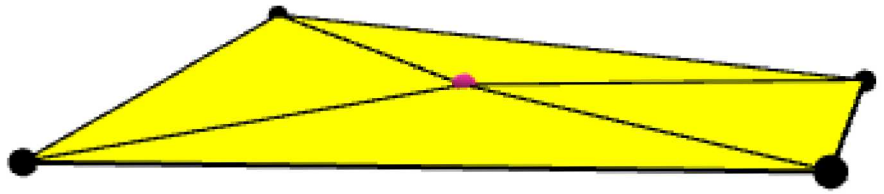

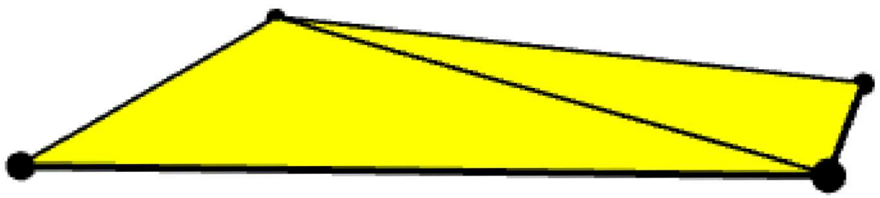

Extra Steiner vertex (sliver) ⇒ No sliver after perturbation of radii

VoroCrust Refinement Loop (revised)

Algorithm 2: High-level VoroCrust algorithm (revised)

Input: Triangle mesh $\mathcal{T}$, and parameters $\theta^\sharp$ and L

```
B ← ∅
while U = ∪B does not cover T do
    Add balls to cover T
    Shrink balls violating any ball conditions
                    or forming half-covered seeds
end
S‡ ← pairs of seeds from triplets of balls in B
return S‡
```

Termination without Slivers

Shrinking violates coverage, requiring new samples

- How much to shrink to uncover $g^{\downarrow}$?

$$\Delta = \frac{r_q - \|q - g^{\downarrow}\|}{r_q} \leq \frac{\|q - g^{\uparrow}\| - \|q - g^{\downarrow}\|}{\|q - g^{\downarrow}\|}$$
$$= \frac{\|q - g^{\uparrow}\|}{\|q - g^{\downarrow}\|} - 1.$$

- Higher sampling density locally flattens the mesh

$$\frac{\|q-g^{\uparrow}\|}{\|q-g^{\downarrow}\|} \to 1 \implies \Delta \to 0$$

- Coverage less likely to be violated with low Δ

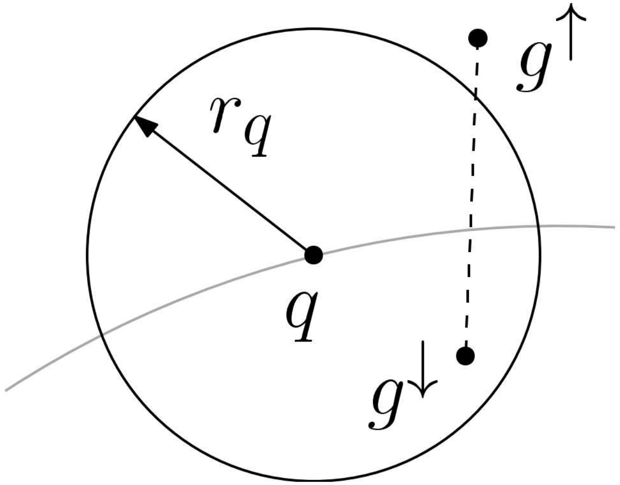

Termination without Slivers

Shrinking violates coverage, requiring new samples

- How much to shrink to uncover $g^{\downarrow}$?

$$\Delta = \frac{r_q - \|q - g^{\downarrow}\|}{r_q} \leq \frac{\|q - g^{\uparrow}\| - \|q - g^{\downarrow}\|}{\|q - g^{\downarrow}\|} = \frac{\|q - g^{\uparrow}\|}{\|q - g^{\downarrow}\|} - 1.$$

- Higher sampling density locally flattens the mesh

$$\frac{\|q-g^{\uparrow}\|}{\|q-g^{\downarrow}\|} \to 1 \implies \Delta \to 0$$

- Coverage less likely to be violated with low Δ

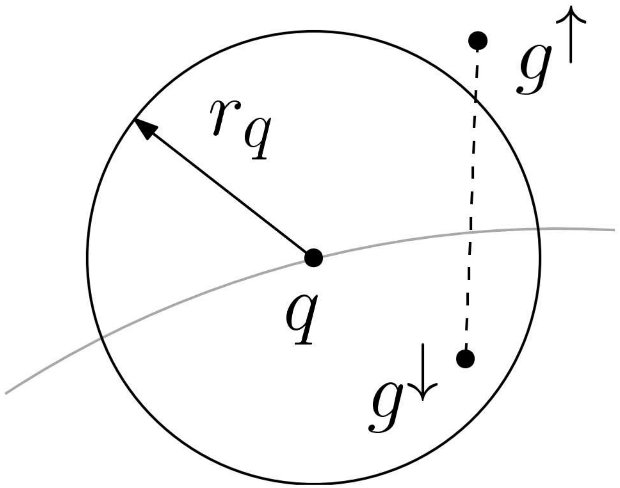

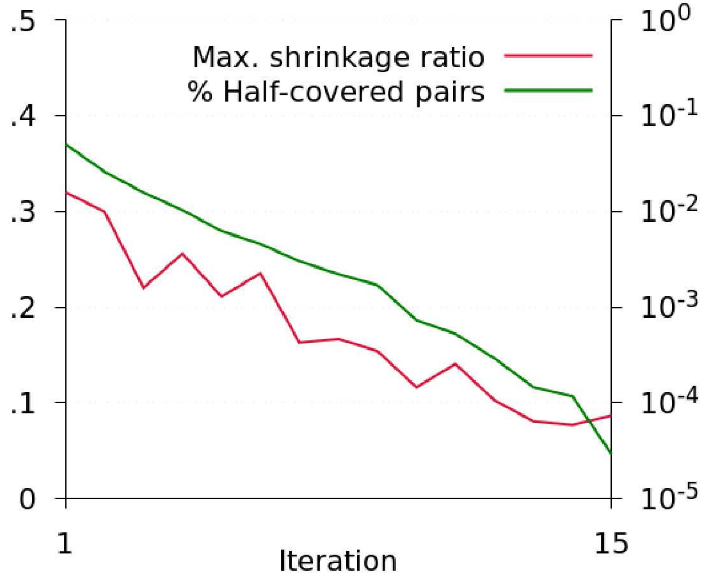

Results: smooth / sharp-features / narrow-regions

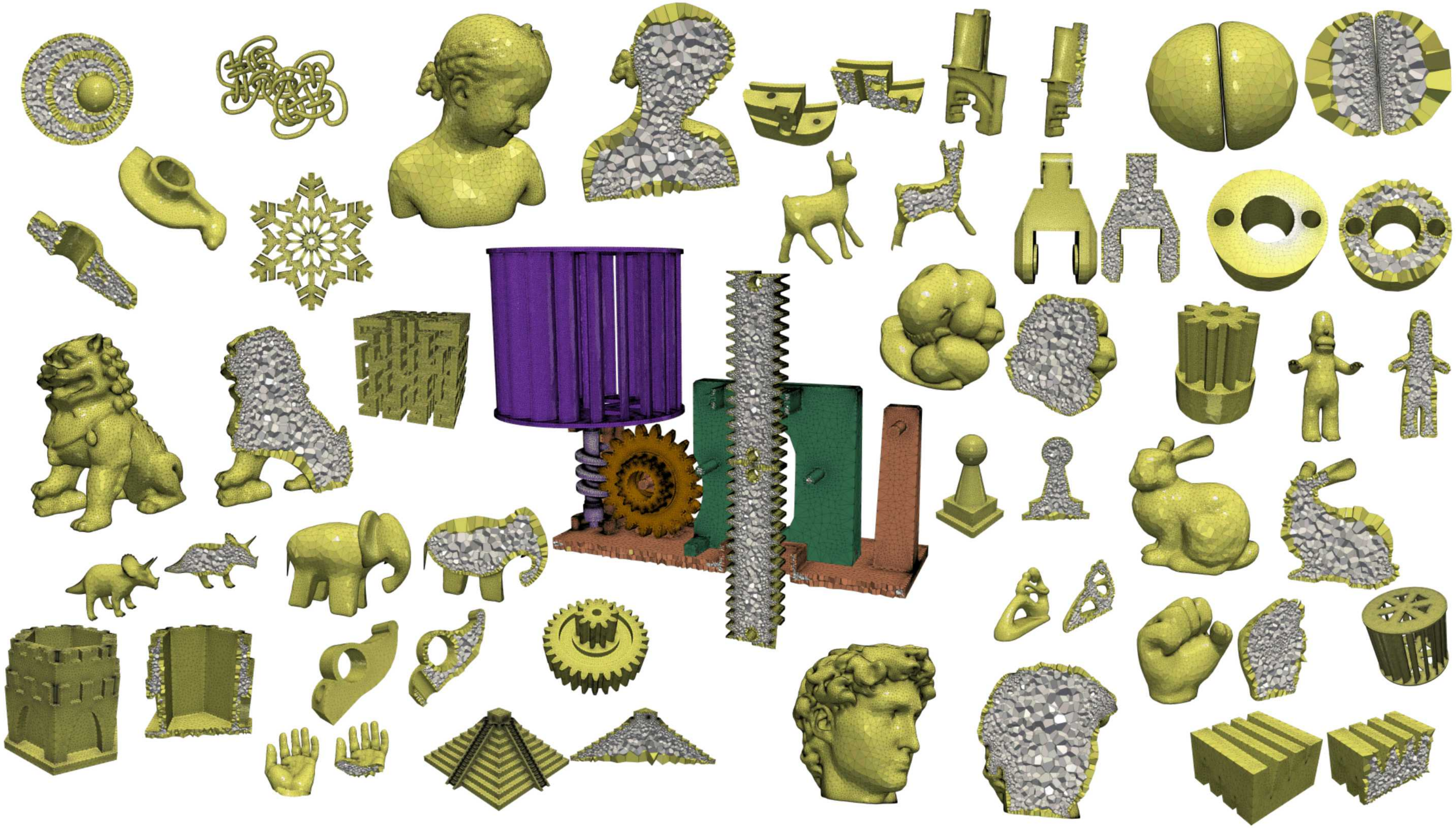

Results: non-manifold

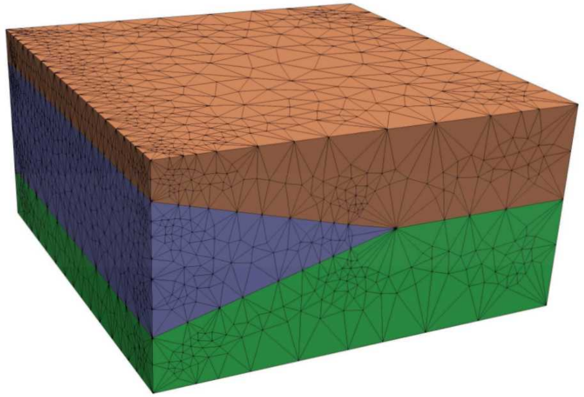

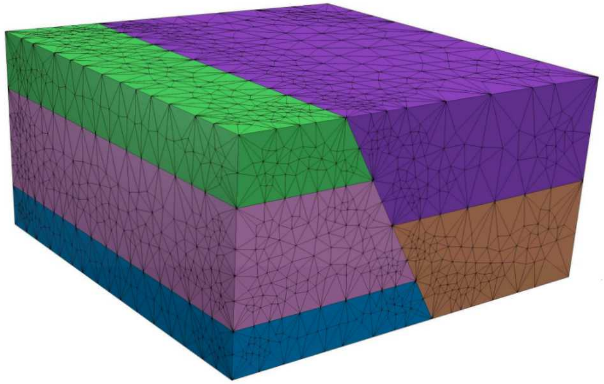

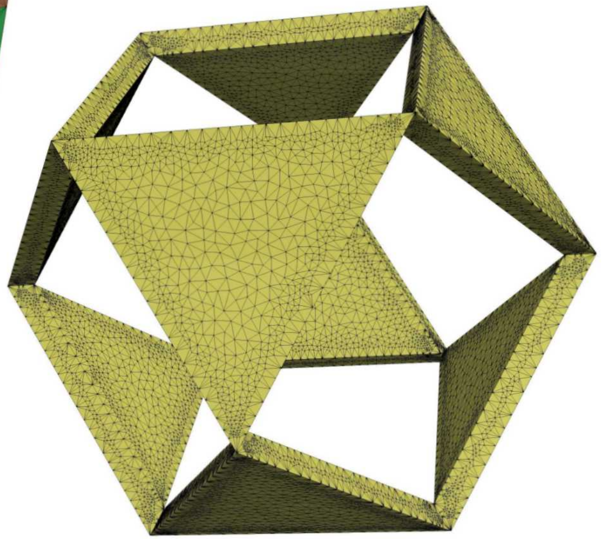

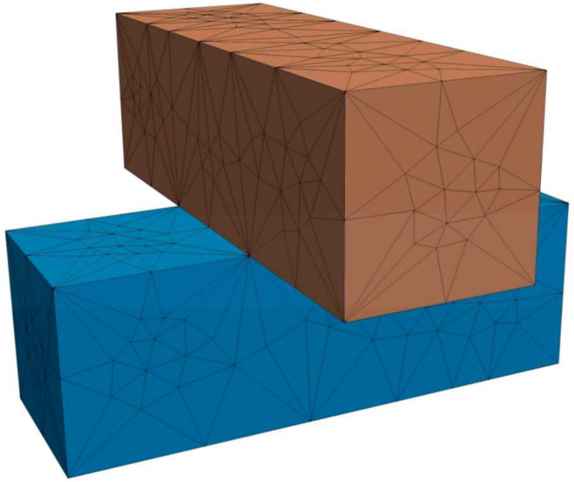

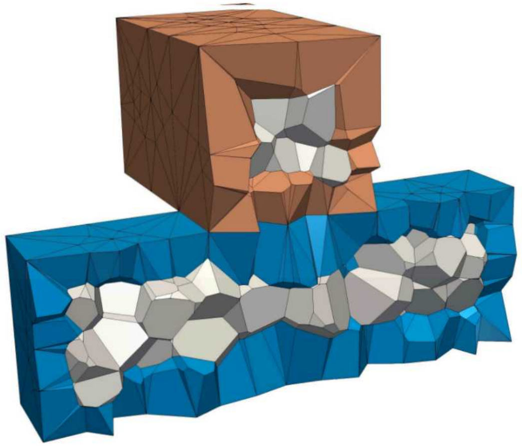

Results: interior

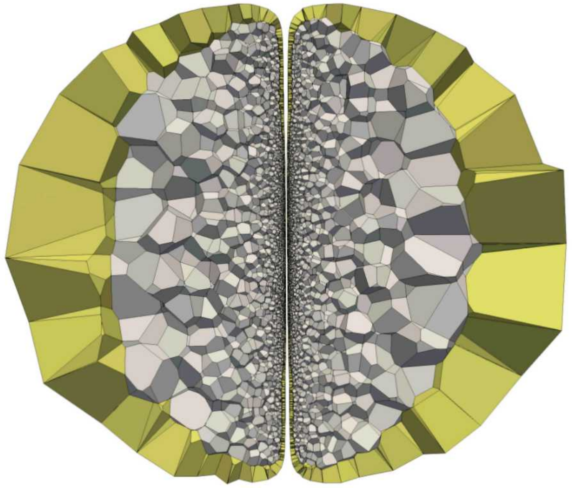

Random

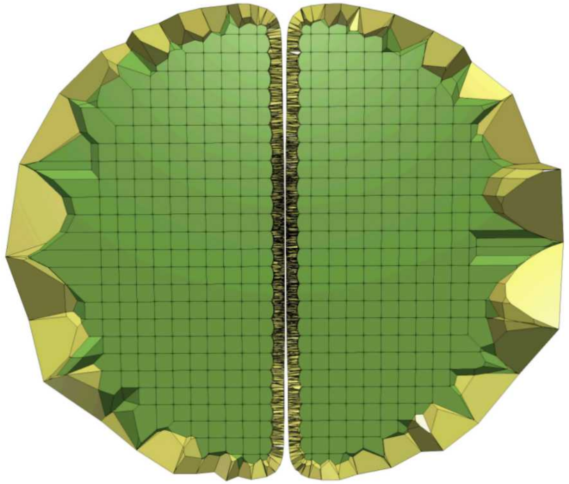

Grid

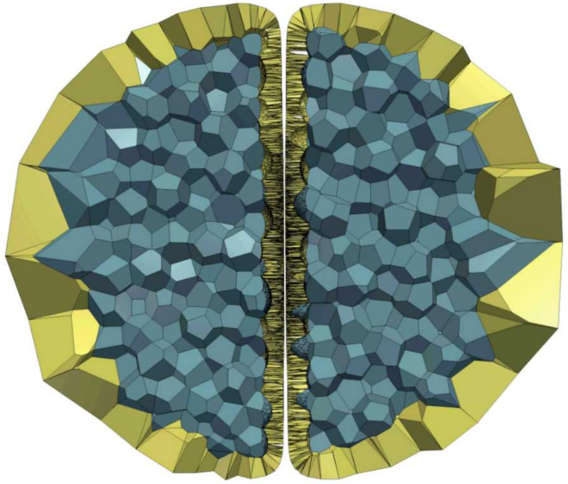

CVT

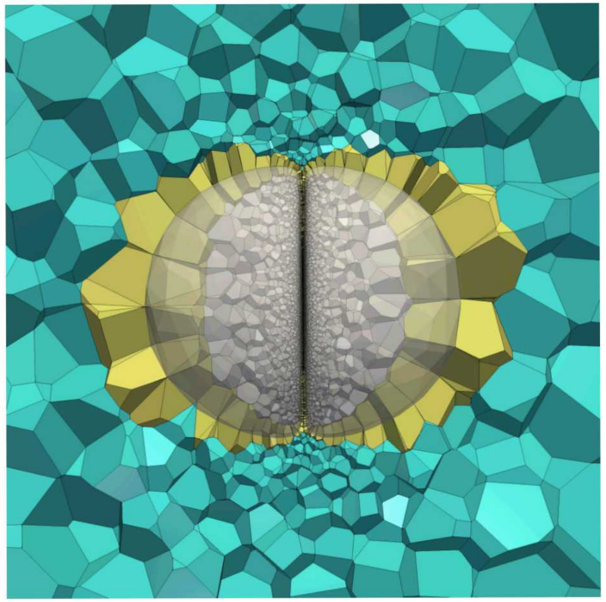

Multi components

Surface Triangle Metrics:

- Minimum triangle quality
- % of angles < 30 or >90
- Hausdorff distance

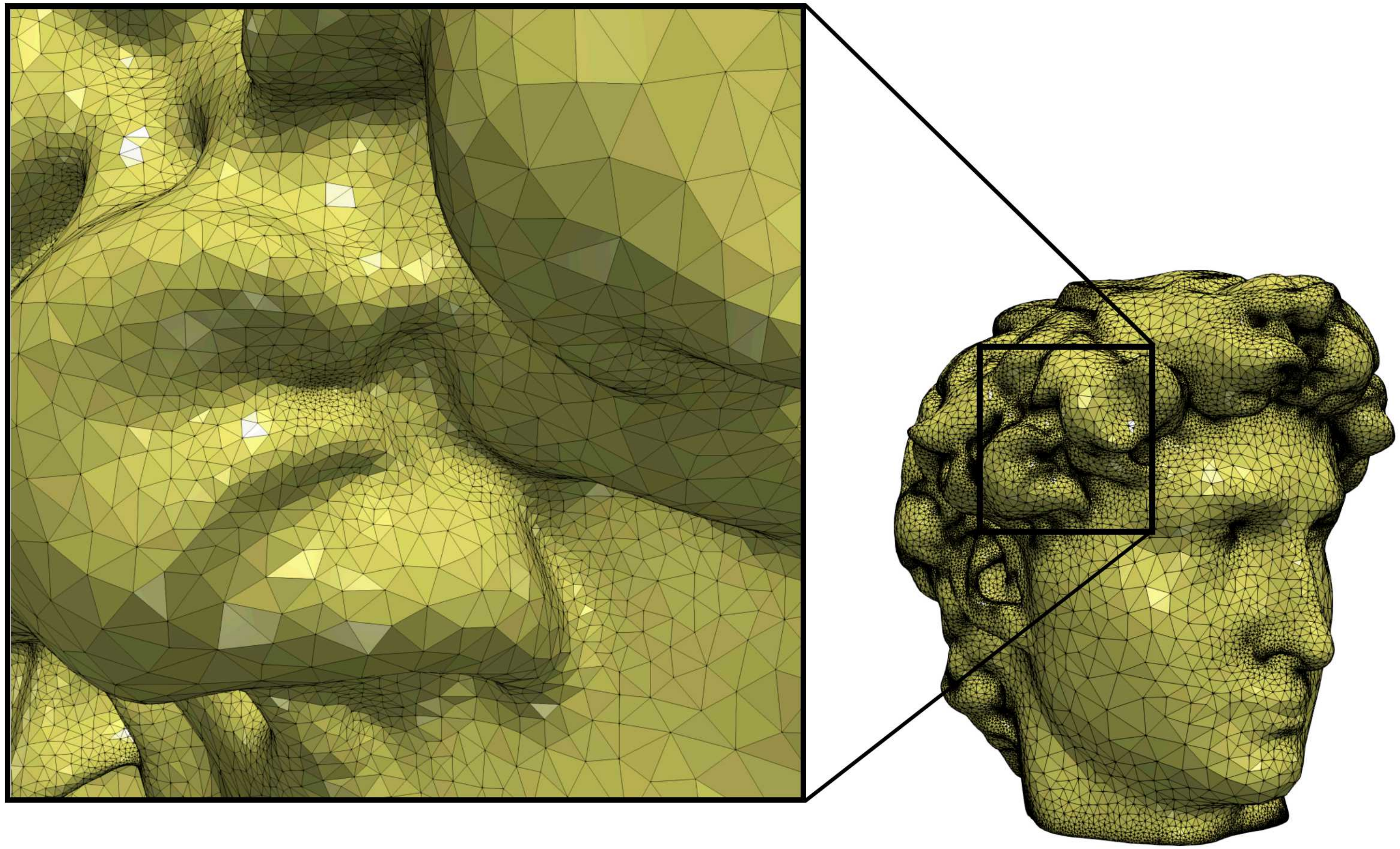

Volume Cells Metrics:

- Maximum aspect ration

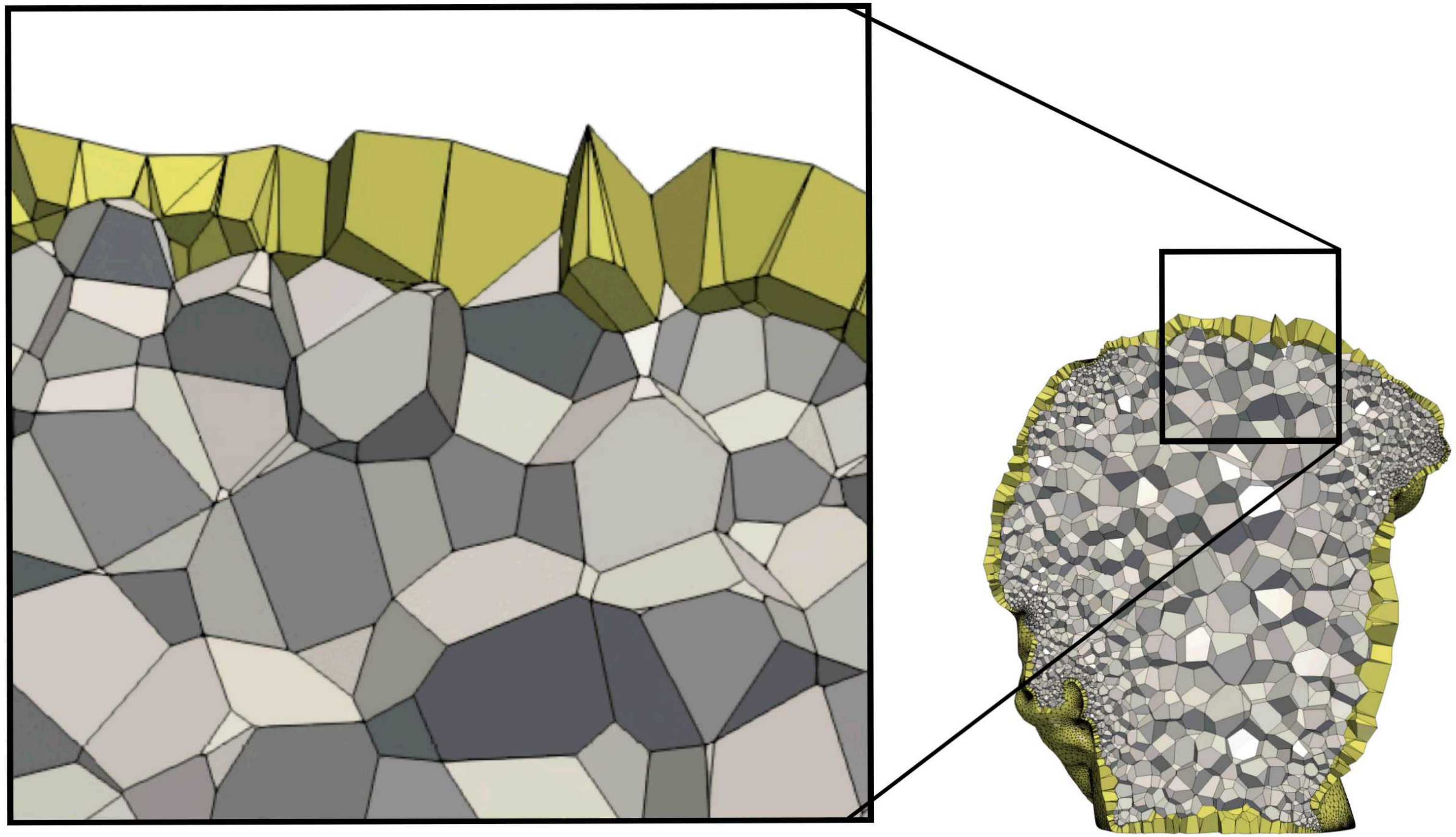

Parameter L:

- Maximum aspect ration

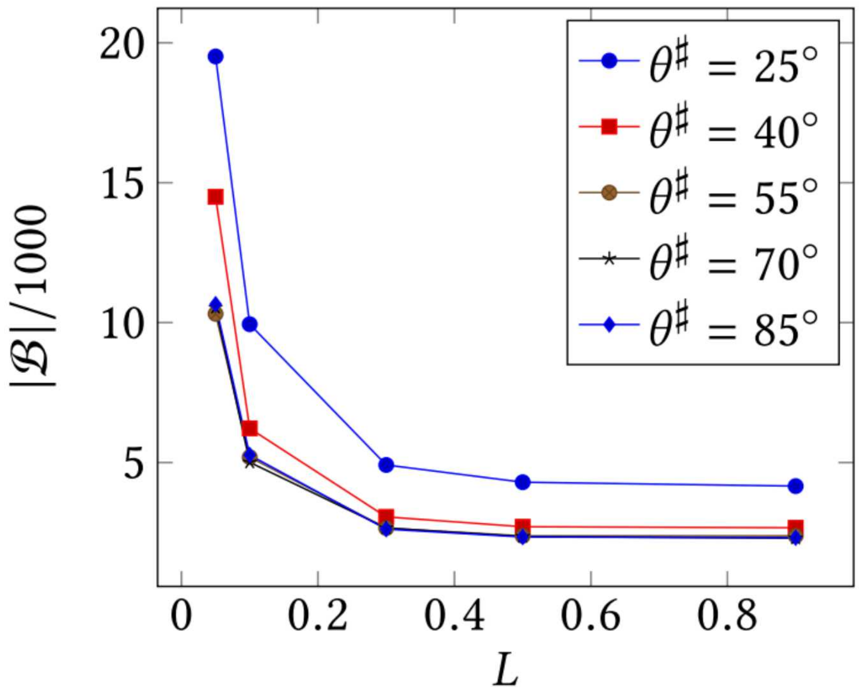

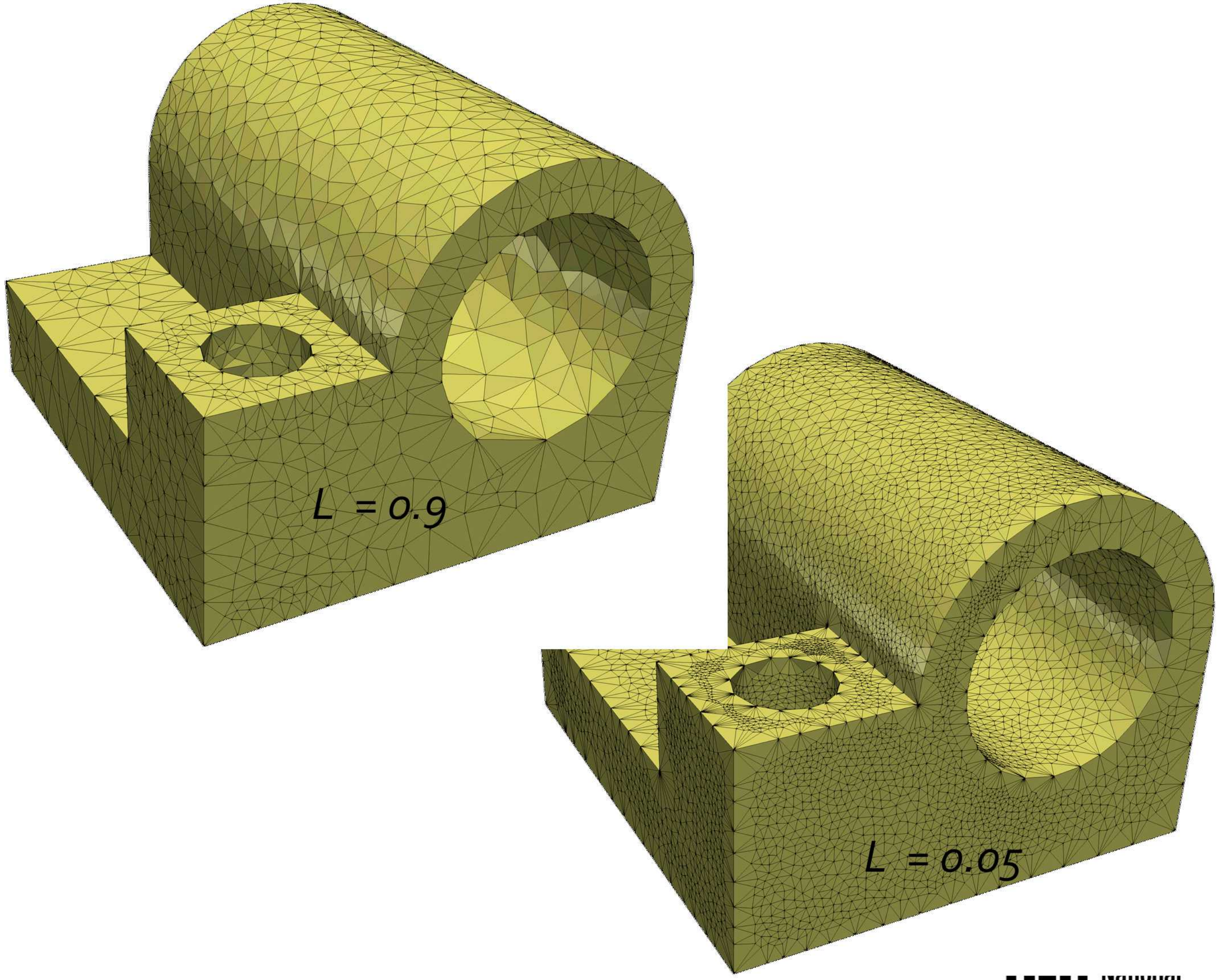

Parameter L

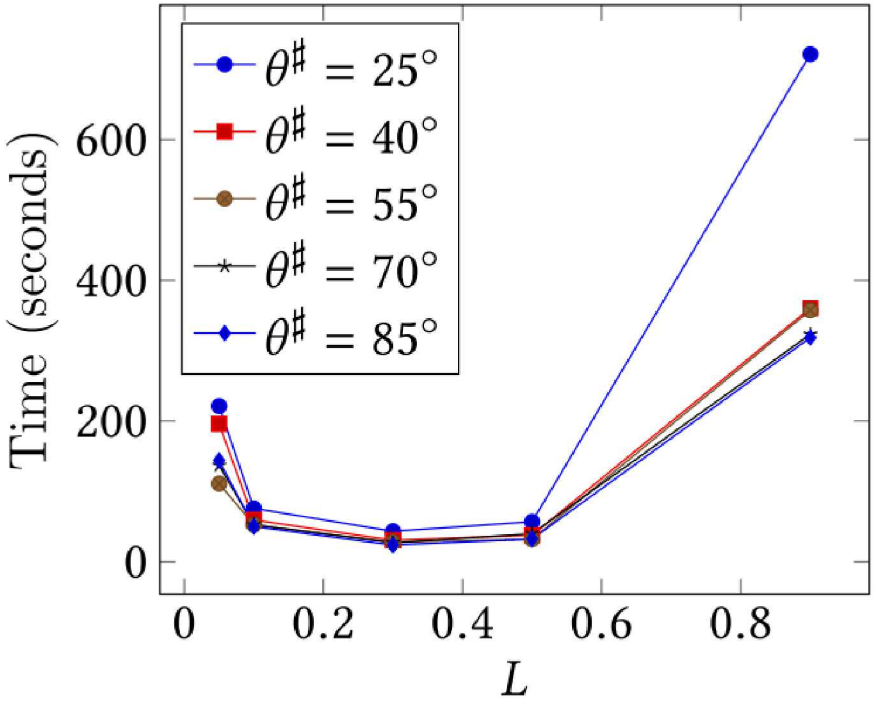

$\theta^\sharp = 25°$
$\theta^\sharp = 40°$
$\theta^\sharp = 55°$
$\theta^\sharp = 70°$
$\theta^\sharp = 85°$
Time (seconds)
0
200
400
600
0
0.2
0.4
0.6
0.8
L

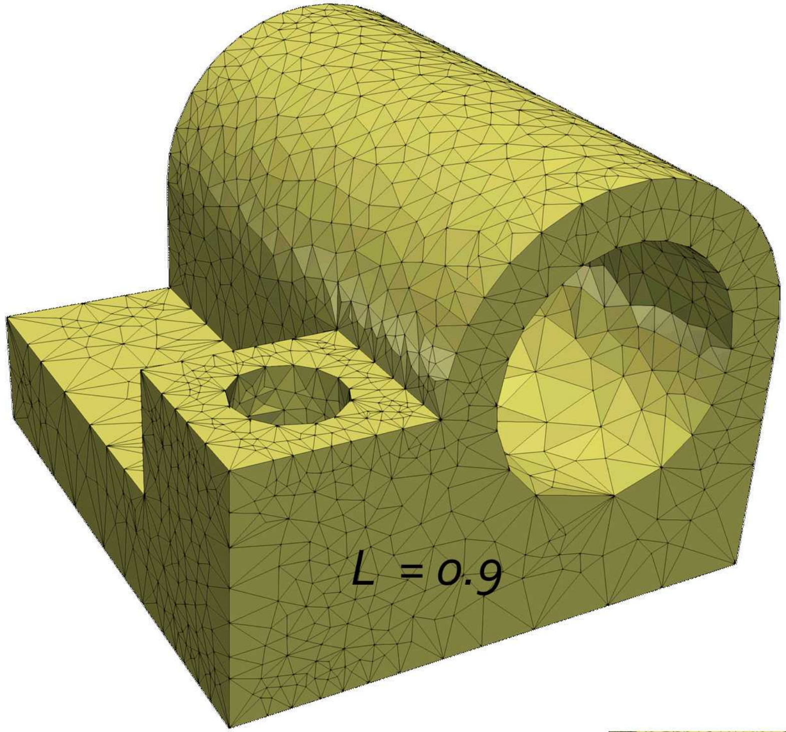

L = 0.9

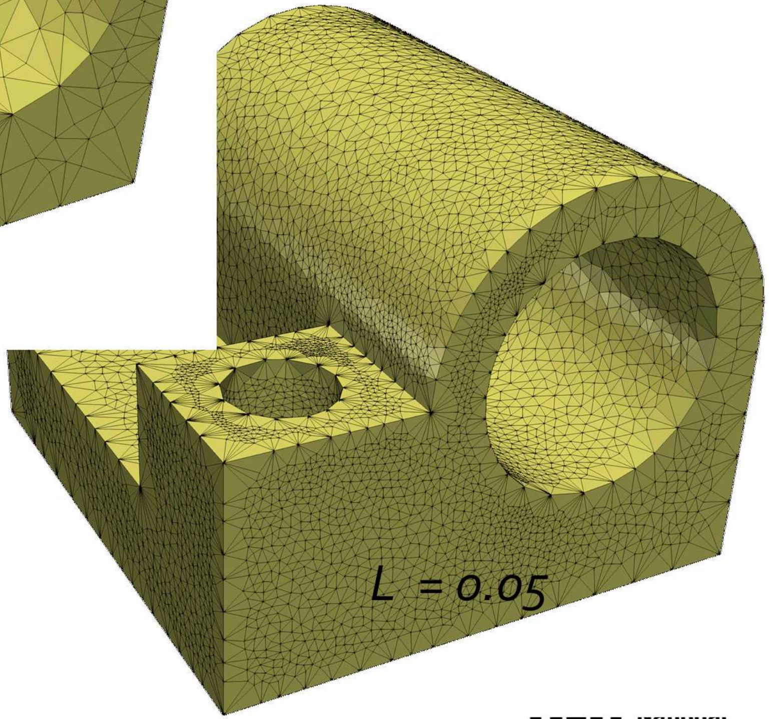

L = 0.05

Results: parameter study

Parameter $(\theta^{\#})$

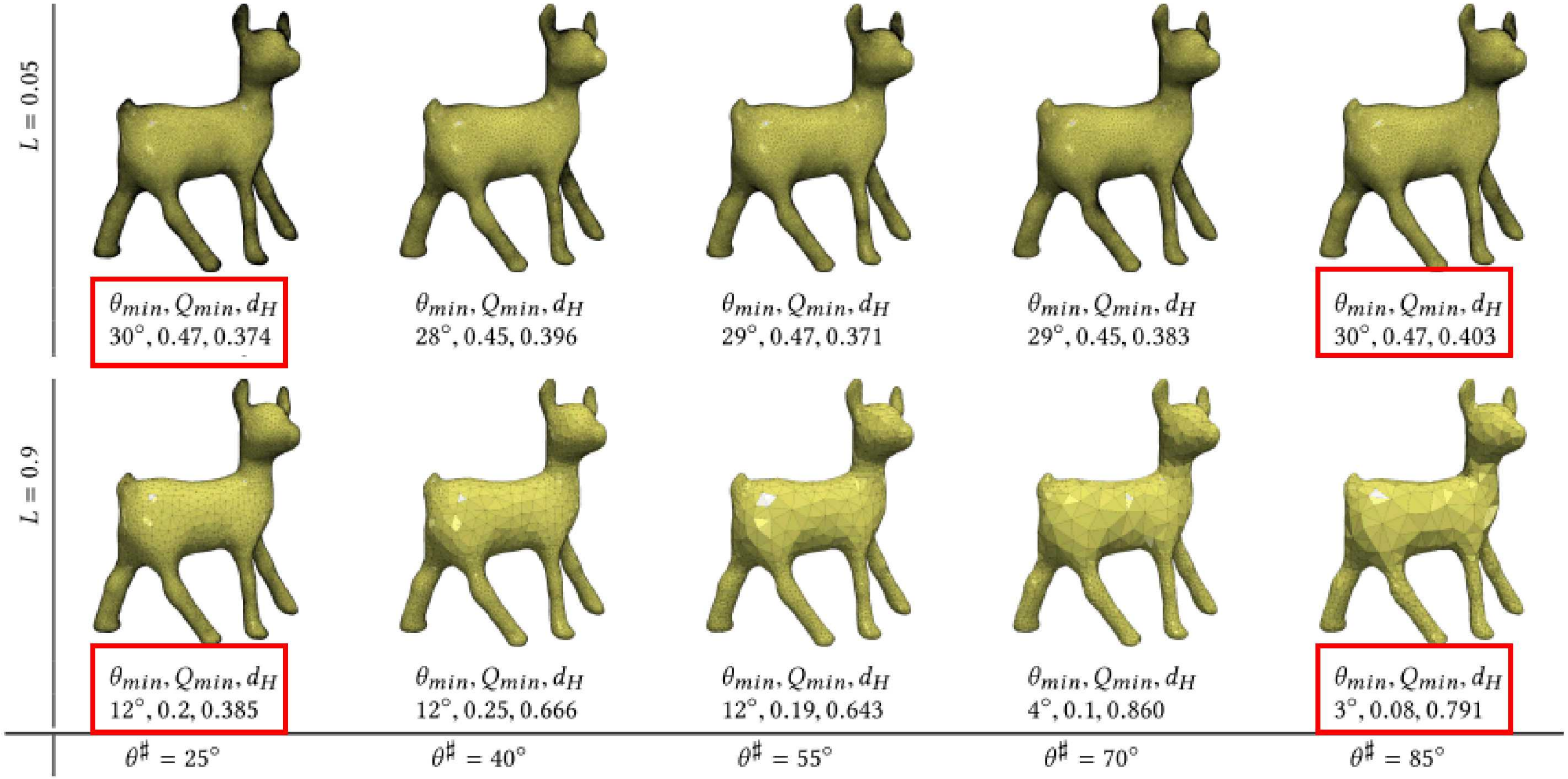

Comparison against Restricted Voronoi Diagram (RVD):

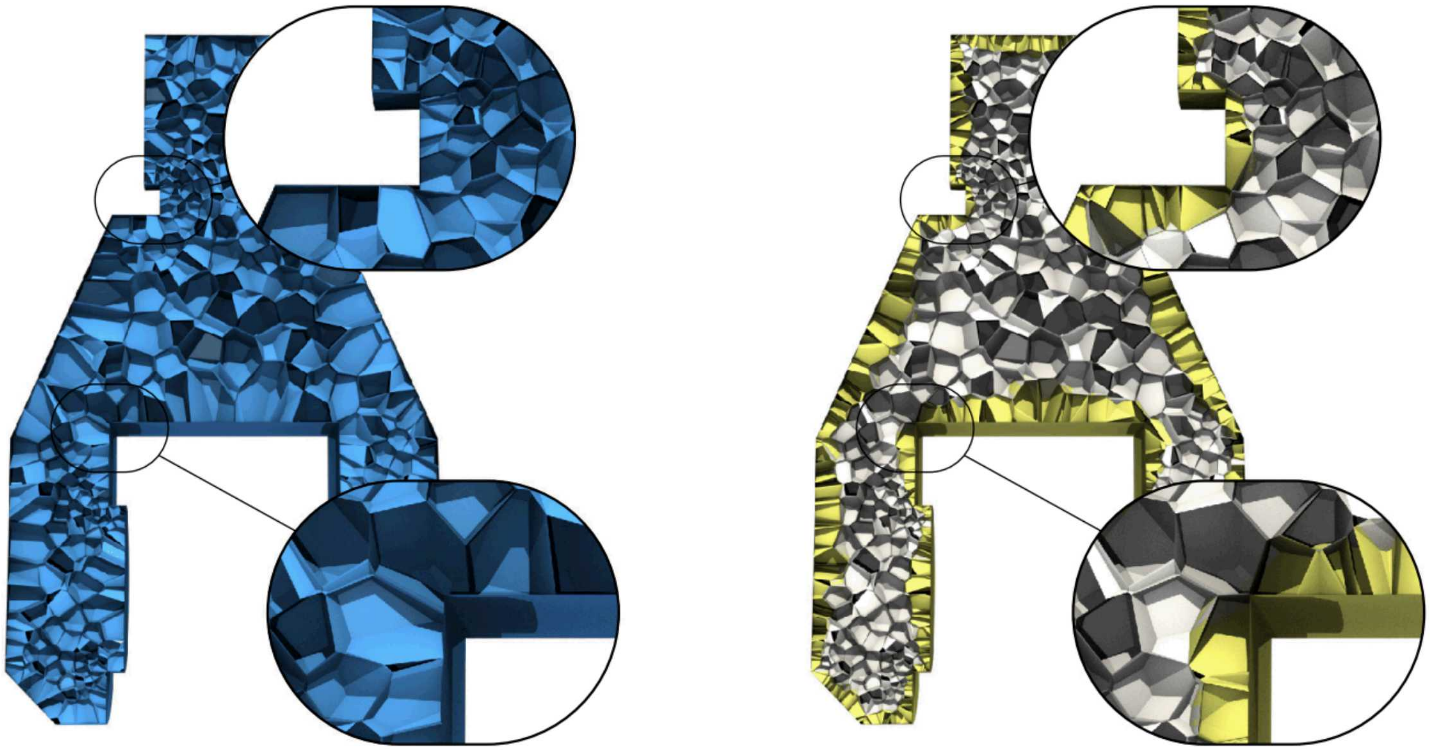

RVD

VoroCrust

Comparison against Restricted Voronoi Diagram (RVD):

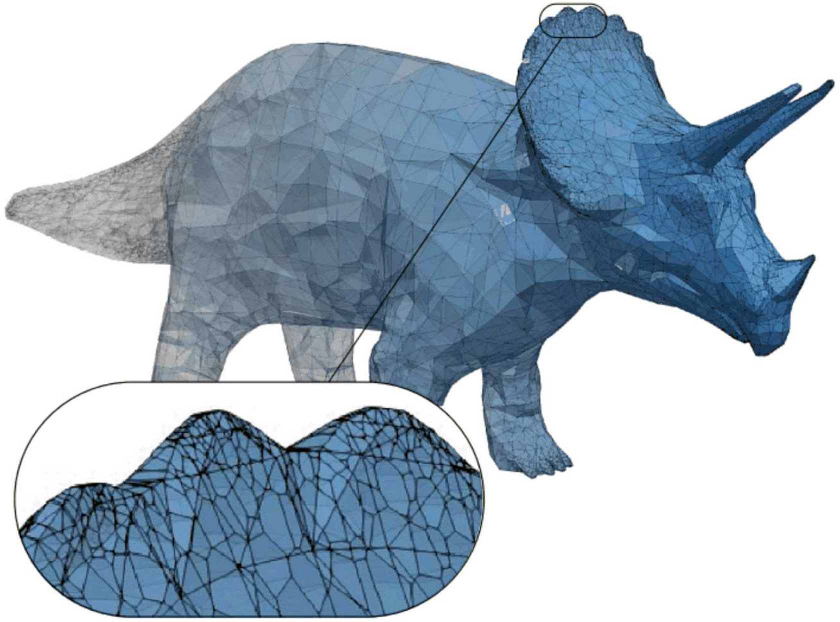

RVD

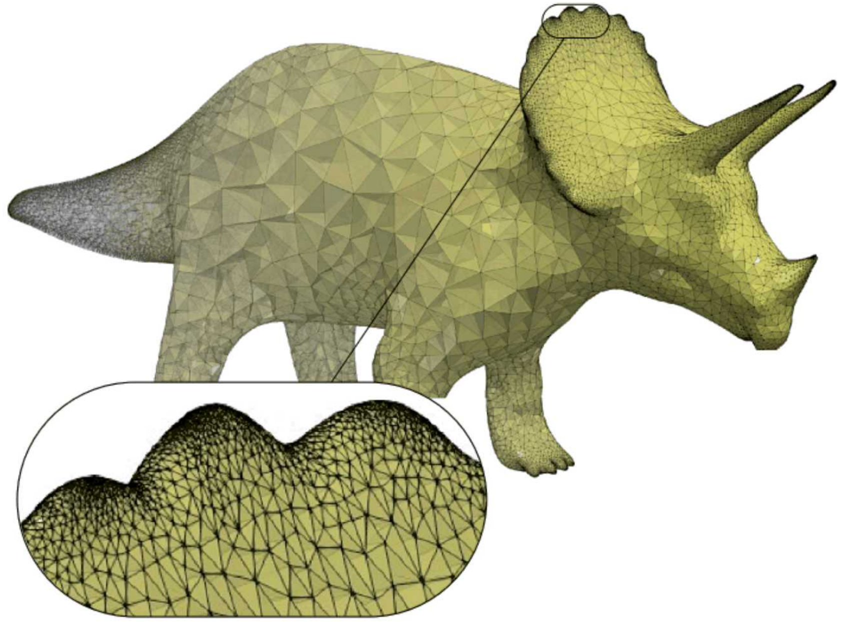

VoroCrust

Comparison against Restricted Voronoi Diagram (RVD):

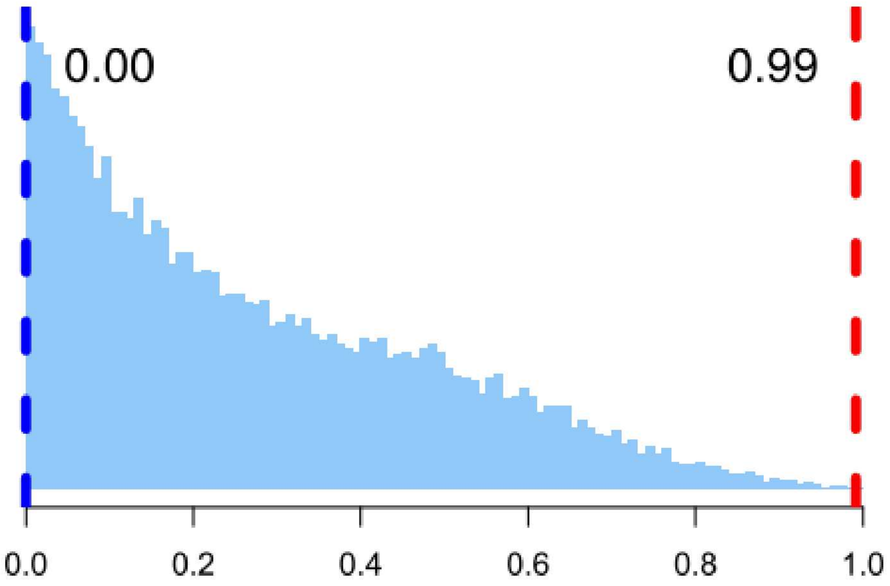

RVD

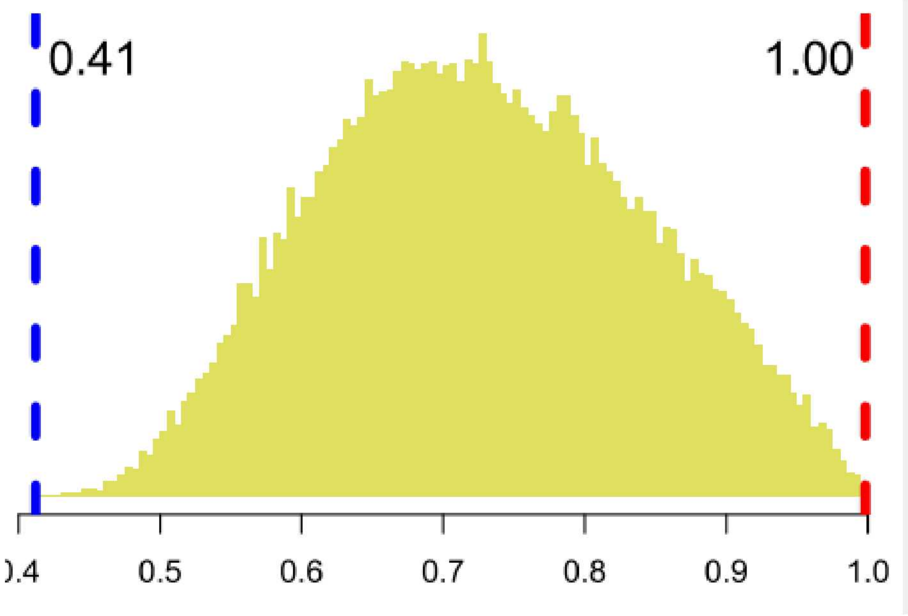

VoroCrust

Limitations

- Short edges
- Input faithfulness (e.g., non-watertight)
- Isotropic sampling

Conclusion

- First provably-correct algorithm for conforming Voronoi mesh on arbitrary domains
- Guarantees on convexity, output quality
- Robust, well-tested implementation
  - VoroCrust.Sandia.gov

Future Work

- Speedup by parallelization
- Anisotropic meshing
- Short edges elimination

Visit

VoroCrust.Sandia.gov

Thank you!

This material was based upon work supported by the U.S. Department of Energy, Office of Science, Office of Advanced Scientific Computing Research (ASCR), Applied Mathematics Program, and the Laboratory Directed Research and Development program (LDRD) at Sandia National Laboratories. Sandia National Laboratories is a multimission laboratory managed and operated by National Technology and Engineering Solutions of Sandia, LLC., a wholly owned subsidiary of Honeywell International, Inc., for the U.S. Department of Energy's National Nuclear Security Administration under contract DE-NA0003525. A. Abdelkader acknowledges the support of the National Science Foundation under grant number CCF-1618866. The research of C. Bajaj was supported in part by the National Institutes of Health under grant number R01GM117594. A. Mahmoud and J. Owens acknowledge the support of the National Science Foundation under grant number CCF-1637442.